

AA 279D GUEST LECTURE

Adam W. Koenig

Stanford's Space Rendezvous Laboratory (SLAB)

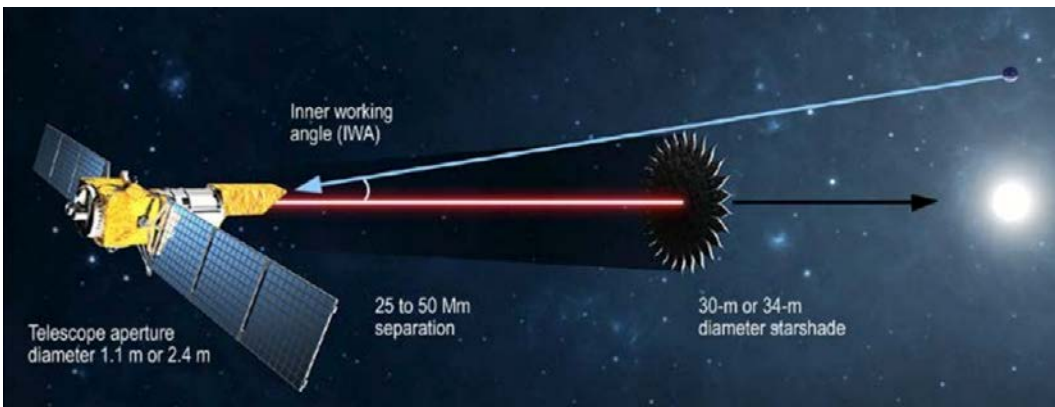
slab.stanford.edu



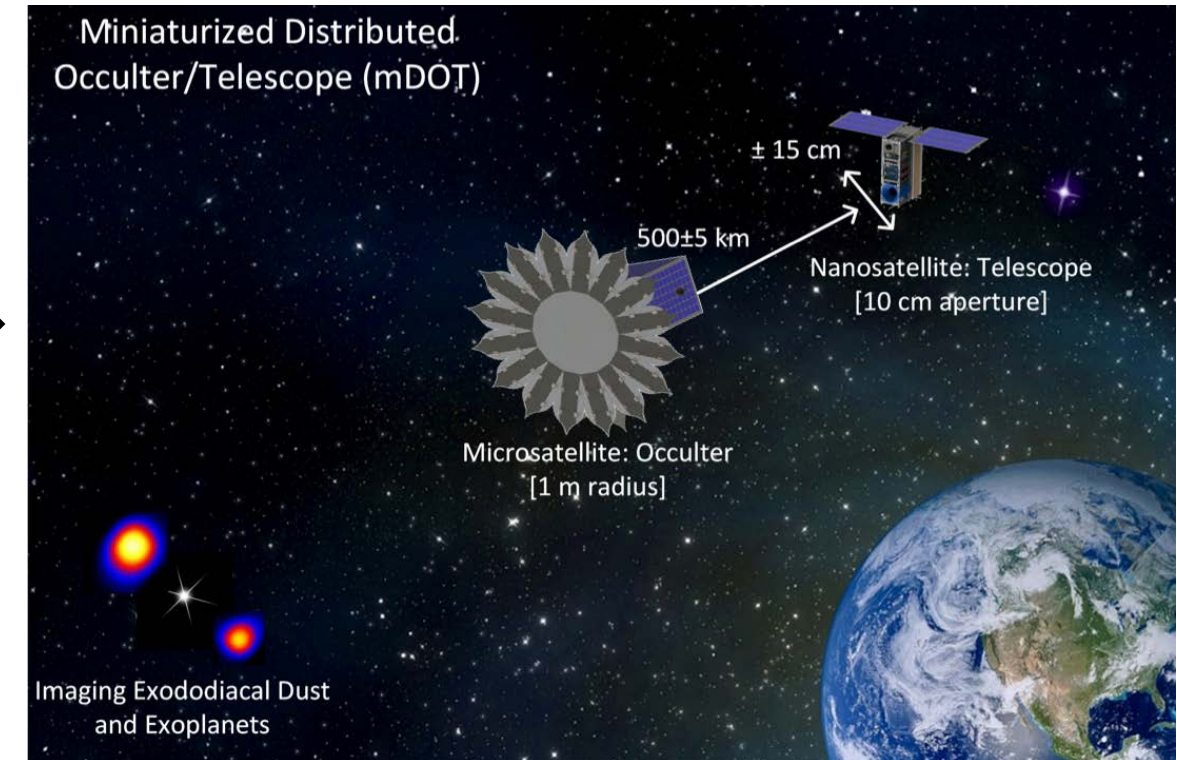
Outline

1. Miniaturized Distributed Occulter/Telescope (mDOT)
 1. Optical Design
 2. Orbit & Operations
2. State transition matrix derivation for perturbed orbits
3. Optimal impulsive control of LTV systems

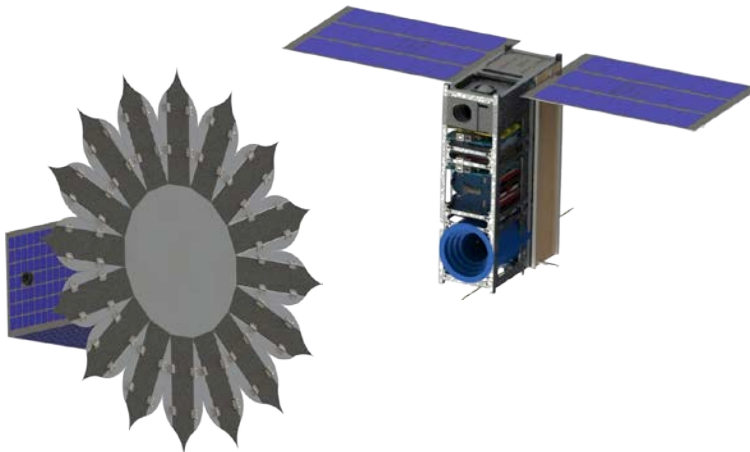
mDOT: High-Contrast Imaging from Earth Orbit



Exo-S Probe-Class Starshade Mission
Credit: MIT/JPL



Motivation



Technology Demonstration

- ↗ Demonstrate starshade contrast performance on orbit
- ↗ Demonstrate autonomous & precise GN&C operations at large separation
- ↗ Develop critical subsystems for full-scale missions

Science

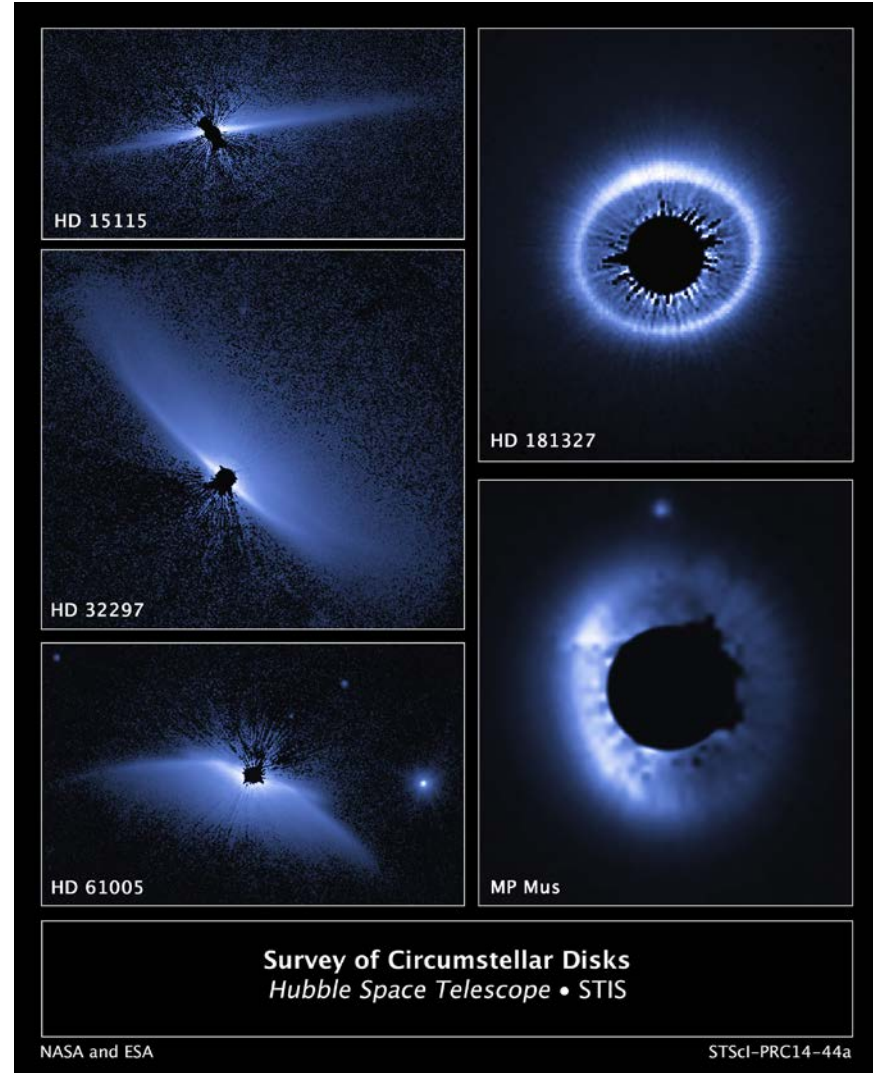
- ↗ Image exozodiacal dust disks and/or large exoplanets
- ↗ Provide complimentary data to earth-based coronagraphs using visible/IR light
- ↗ Characterize environment around nearby stars

mDOT Optics: Key Questions

- 1. What scientifically relevant targets can be seen with small telescopes?**
- 2. Can starshades be miniaturized to enable deployment in Earth orbit?**

mDOT Optics: Key Questions

- ↗ Exozodii
 - ↗ Dust disks surrounding other stars
 - ↗ Can be multiple orders of magnitude brighter than Milky Way
- ↗ Jovian exoplanets
 - ↗ Jupiter-sized planets orbiting close to their parent star



mDOT Optics: Key Questions

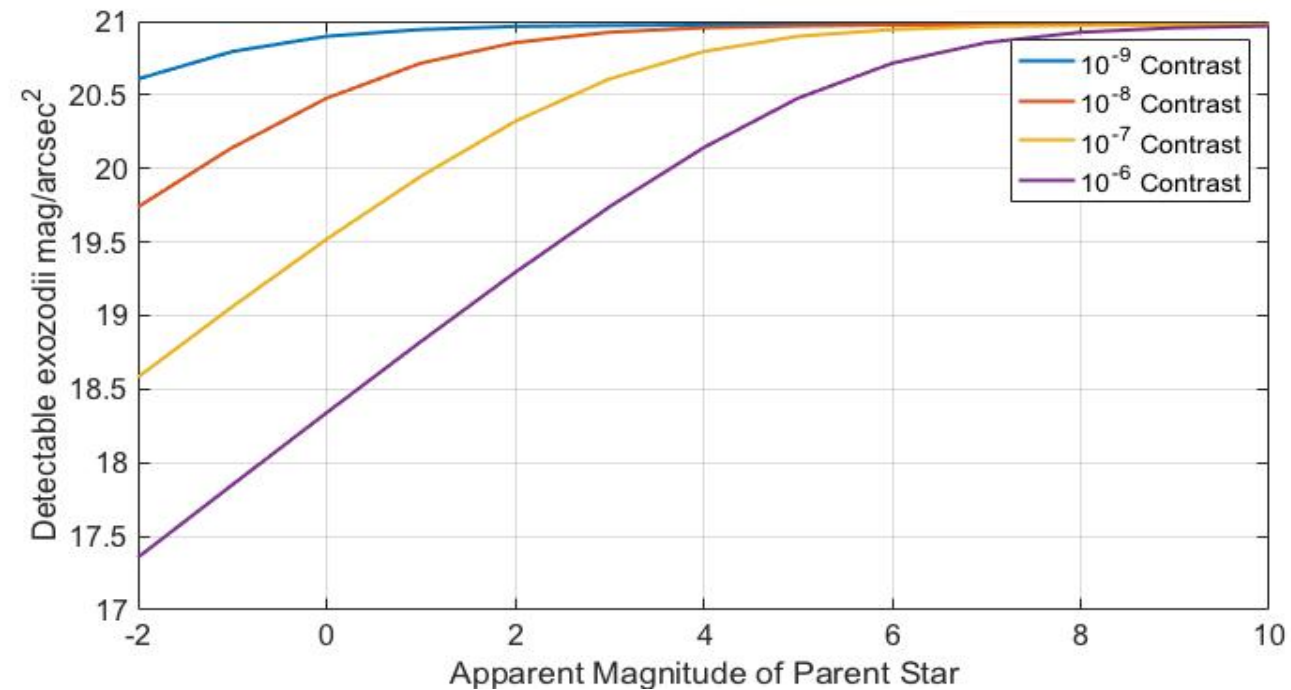
- ↗ Exozodii
 - ↗ Dust disks surrounding other stars
 - ↗ Can be multiple orders of magnitude brighter than Milky Way
- ↗ Jovian exoplanets
 - ↗ Jupiter-sized planets orbiting close to their parent star



Credit: Gemini Planet Imager

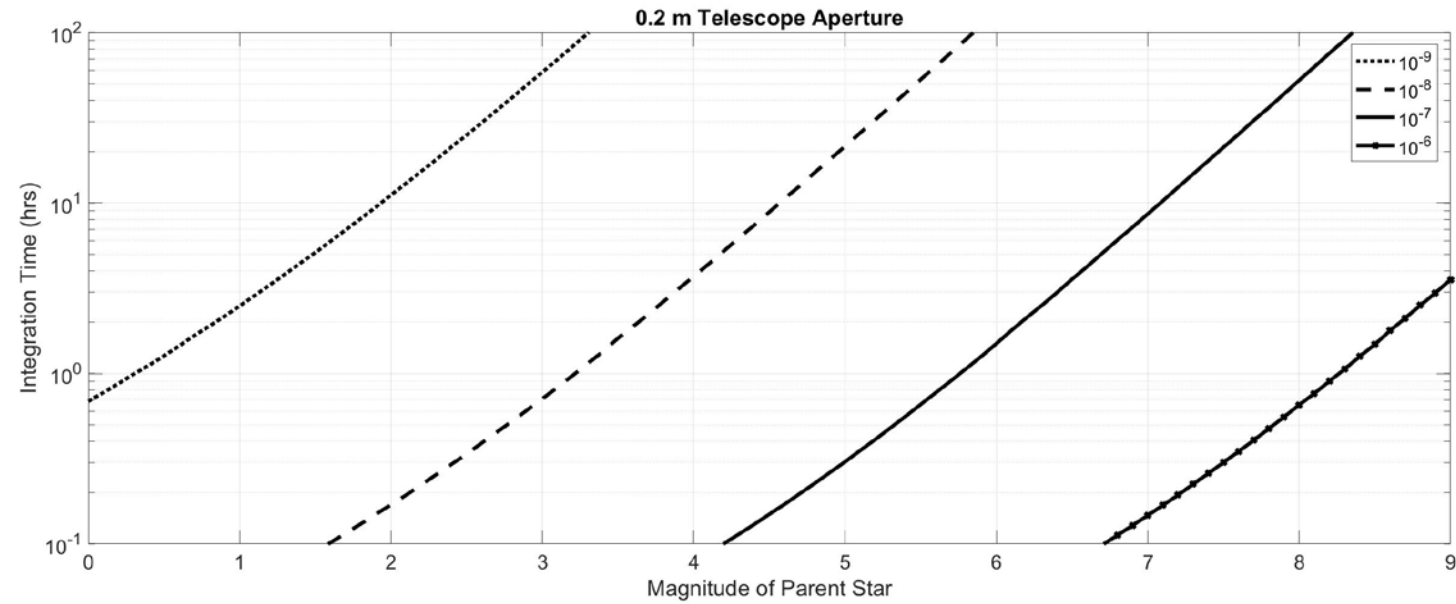
mDOT Optics: Telescope Sizing

- ↗ Exozodii assumptions
 - ↗ 10 cm telescope
 - ↗ B-band spectrum
 - ↗ 5 min integration time
- ↗ Results
 - ↗ Can image dust disks up to 10 mag/argsec²



mDOT Optics: Telescope Sizing

- ↗ Exoplanet assumptions
 - ↗ 20 cm telescope
 - ↗ B-band spectrum
 - ↗ 1.5 hr science phases
- ↗ Results
 - ↗ Need bright star ($B < 5$)
 - ↗ Can image Jovian planets



mDOT Optics: Key Questions

1. What scientifically relevant targets can be seen with small telescopes?
2. **Can starshades be miniaturized to enable deployment in Earth orbit?**

mDOT Optics: Starshade Design

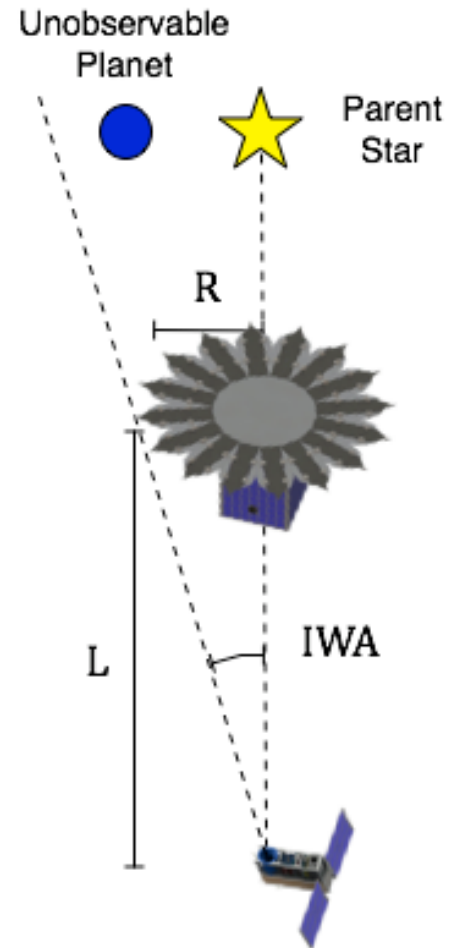
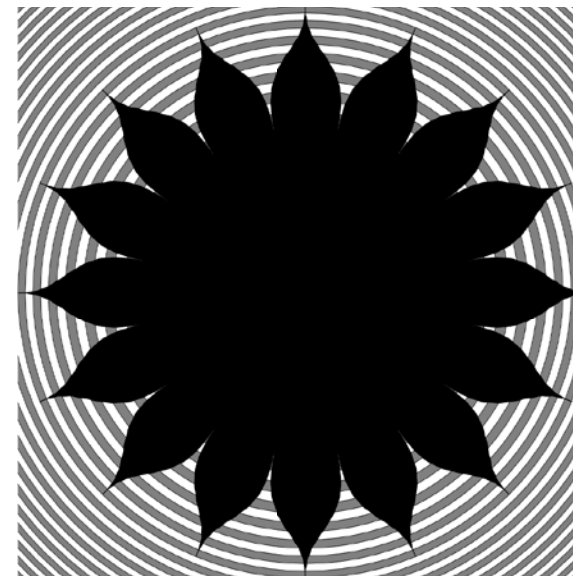
- ↗ Objective:
 - ↗ Minimize inter-spacecraft separation without compromising starshade optical performance

- ↗ Two key variables:
 - ↗ Inner working angle (IWA)

$$IWA = \frac{R}{L}$$

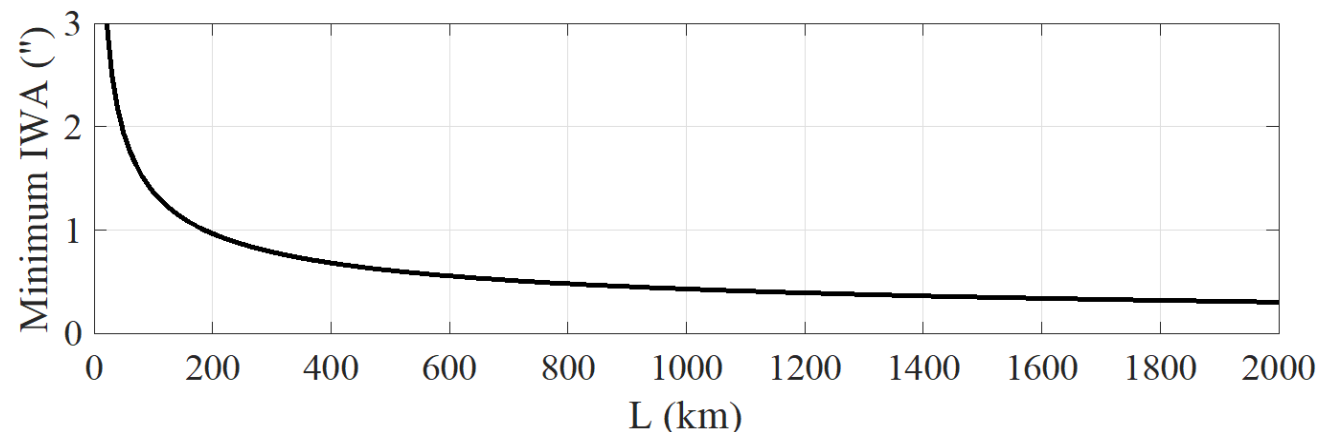
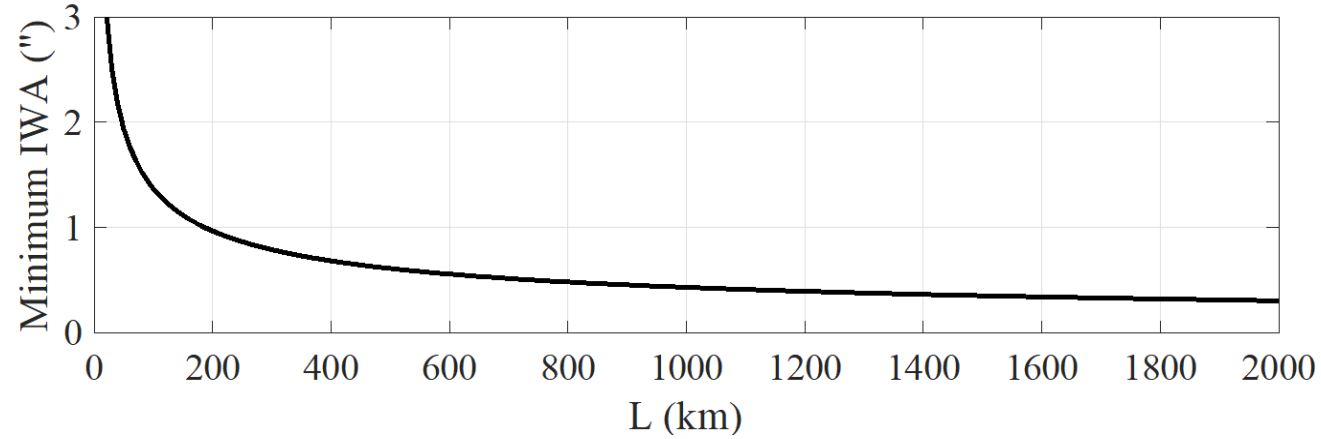
- ↗ Fresnel number

$$F = \frac{R^2}{L\lambda} = IWA^2 \frac{L}{\lambda}$$



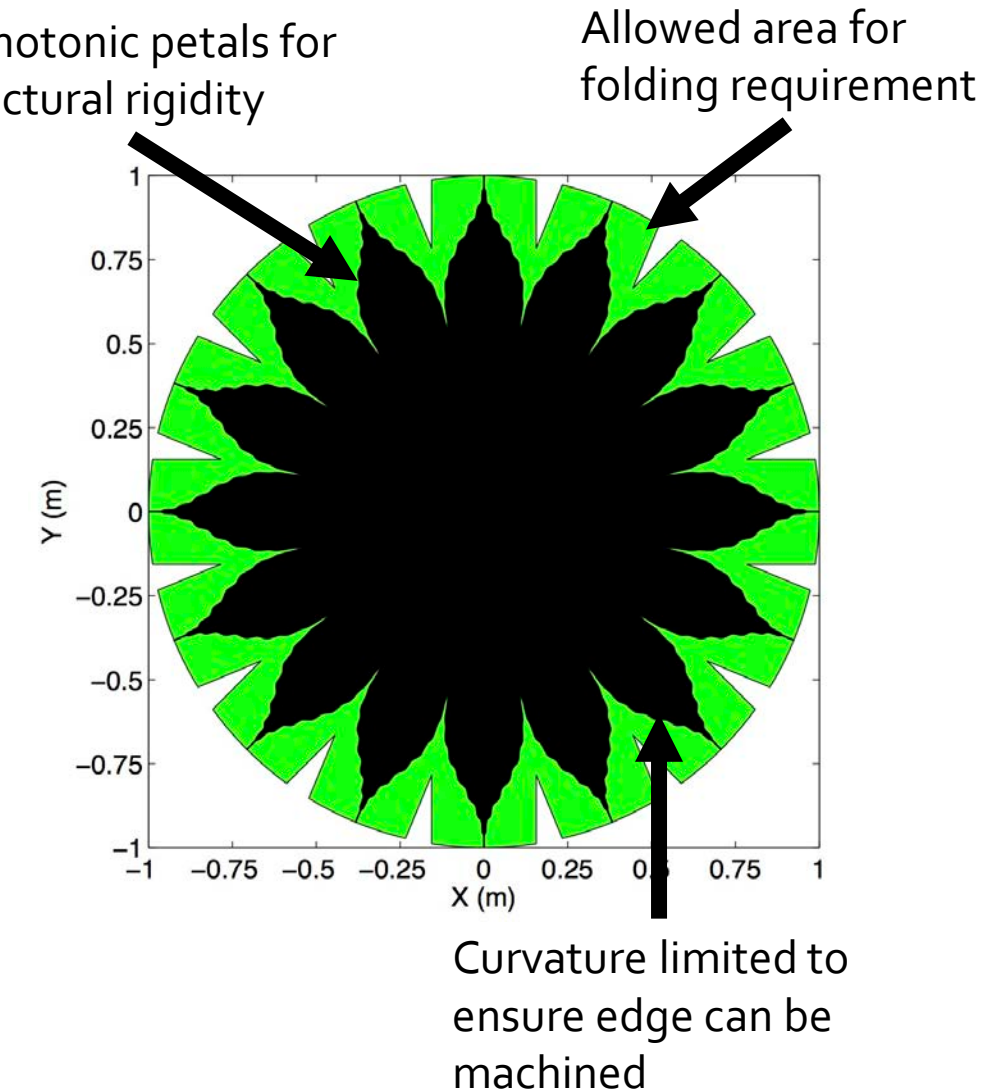
mDOT Optics: Starshade Design

- ↗ Two ways to decrease L at constant Fresnel number
 - 1. Decrease λ to B-band (440 nm)
 - 2. Increase IWA to hundreds of mas

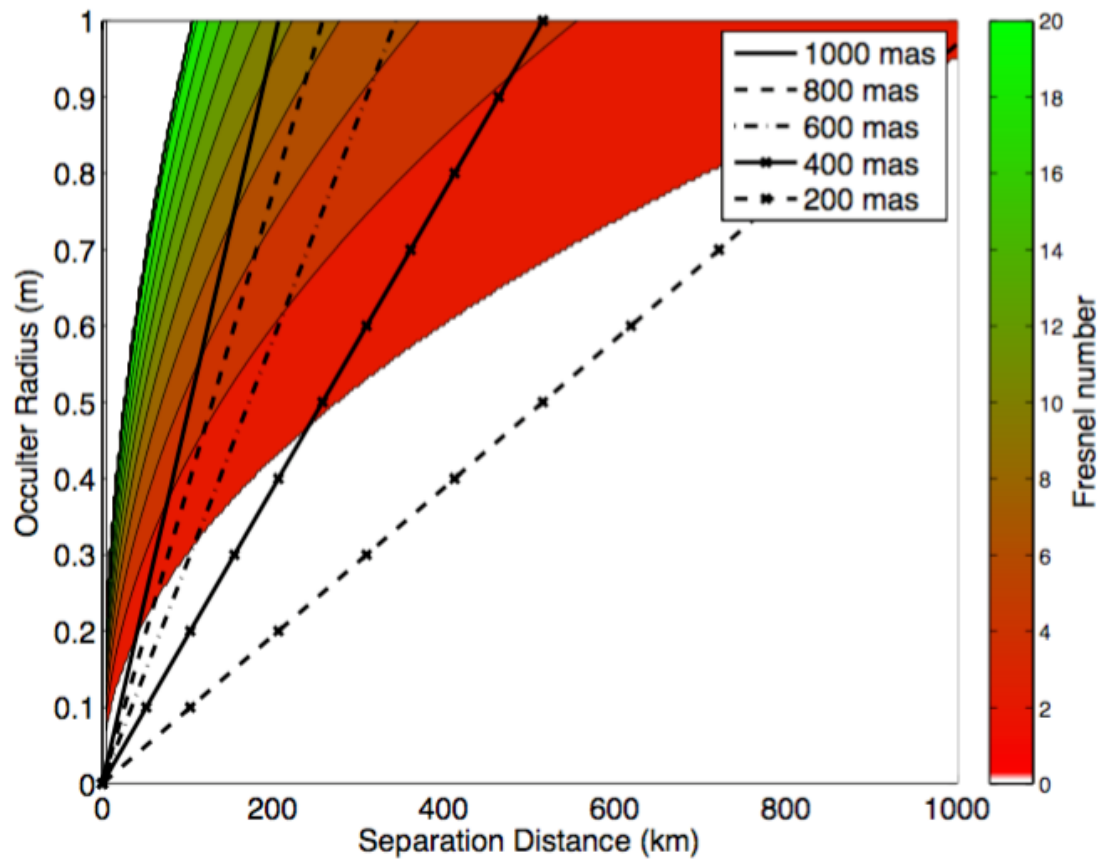


mDOT Optics: Starshade Design

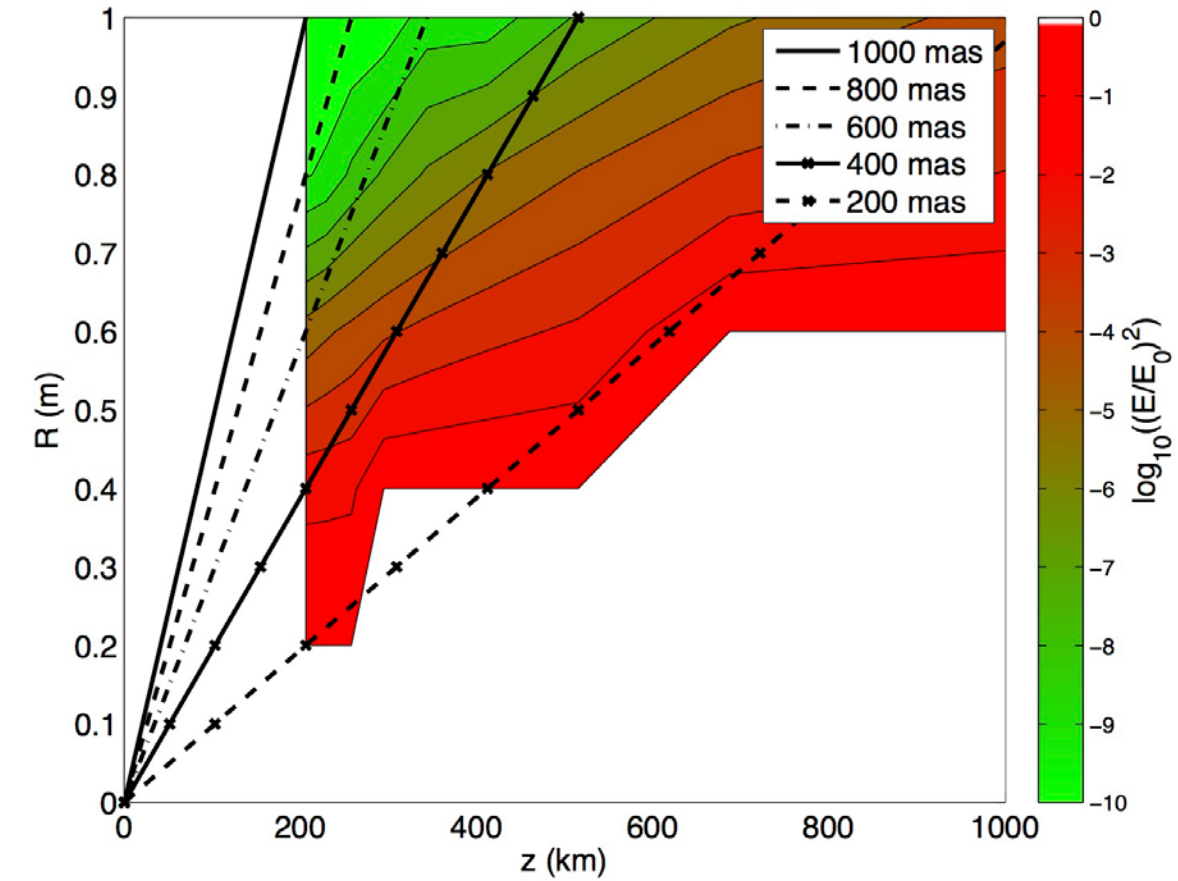
- ↗ Petal shape determined by convex optimization problem
- ↗ Objective: Minimize light intensity in shadow
- ↗ Constraints:
 1. Petal width decreases monotonically
 2. Curvature of petals less than specified limit
 3. Petals can be folded



mDOT Optics: Starshade Design

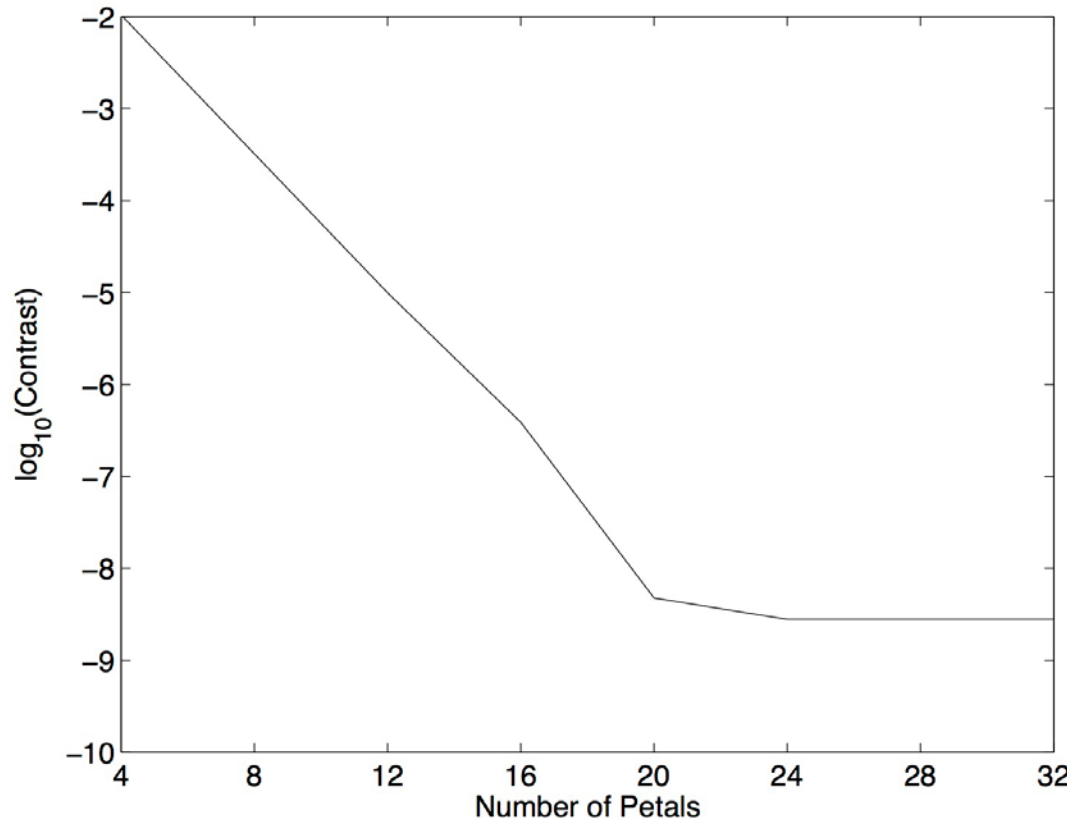


Fresnel Number

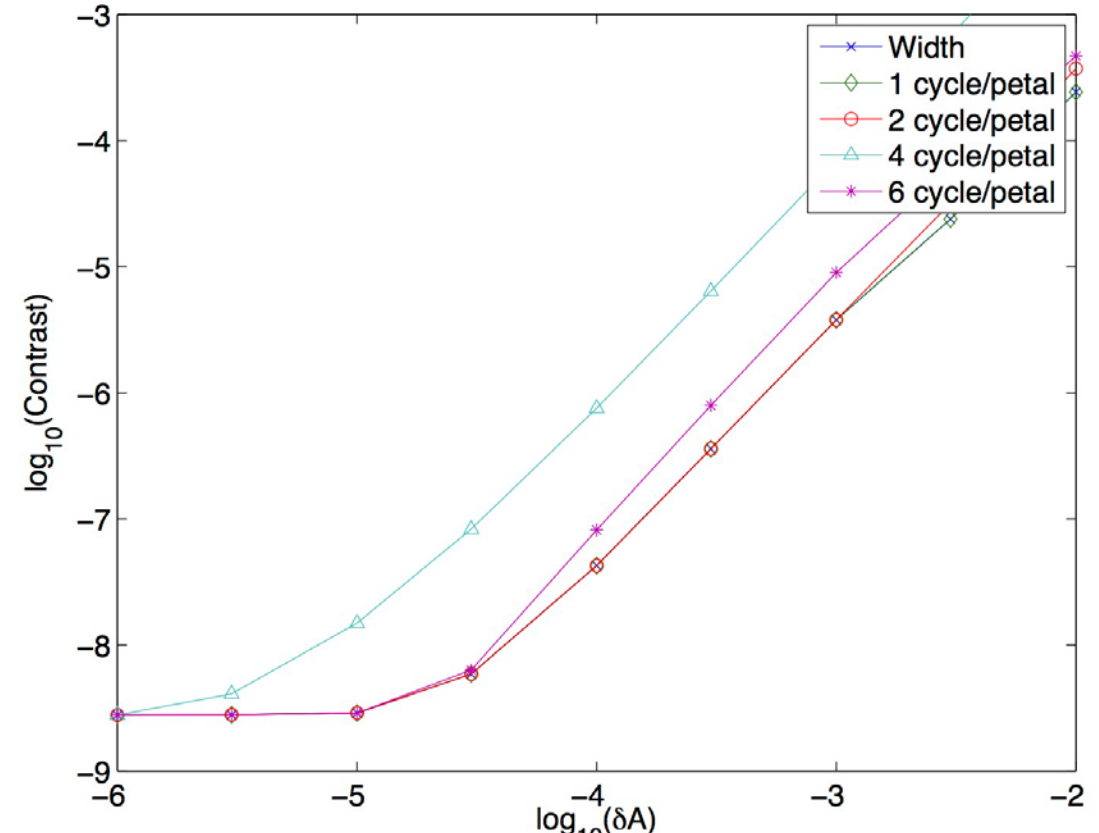


Starshade Light Suppression

mDOT Optics: Starshade Design



Starshade contrast vs number of petals



Starshade contrast with perturbations

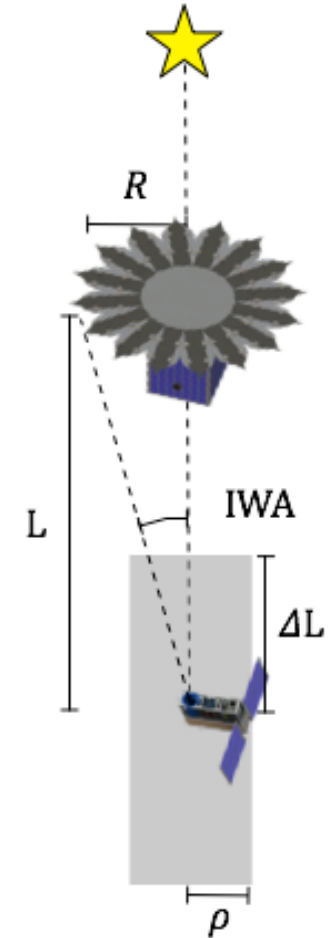
mDOT Optics Review

1. Small (10-20 cm) telescopes can image scientifically interesting targets
2. Starshade can be miniaturized enough to be deployed in earth orbit
3. Miniaturized starshade is realizable with tolerances of at least 1 micron

mDOT Orbit & Operations

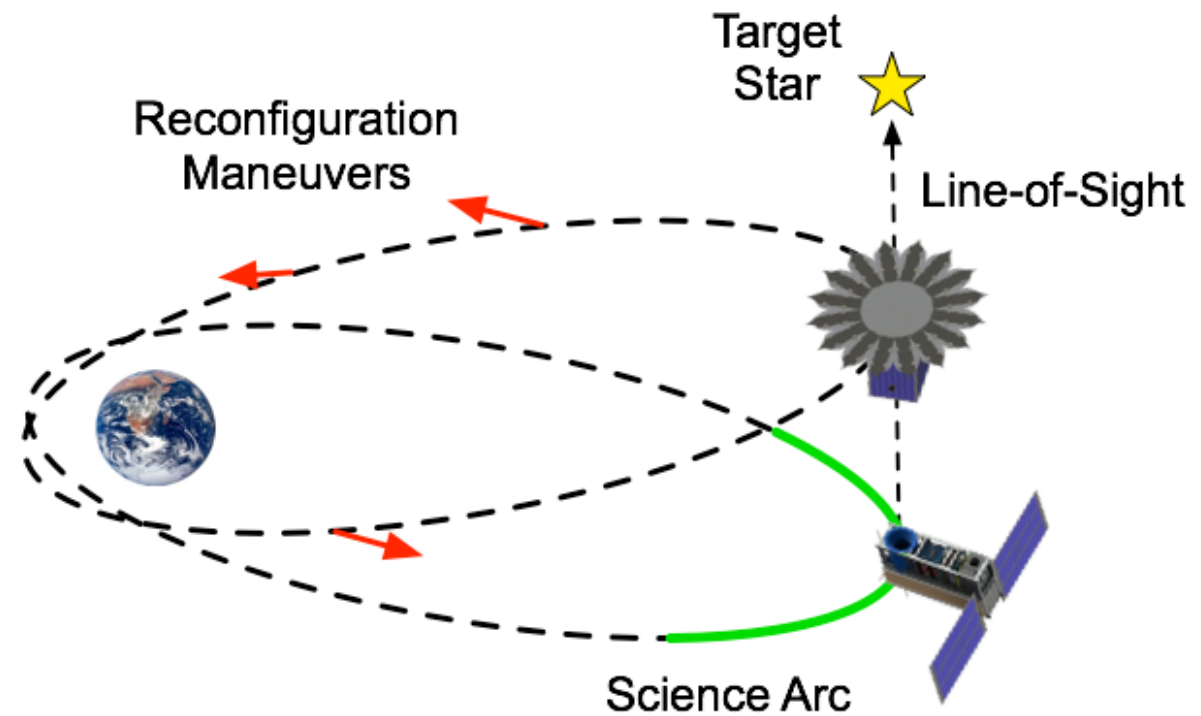
- ↗ Objective: Minimize delta-v cost required to maintain precise alignment with inertial target(s)
- ↗ Challenge: Relative accelerations in Earth orbit are orders of magnitude larger than at L₂
- ↗ **Solution: Exploit insensitivity of starshade performance to separation**

Starshade shadow at least several km in length



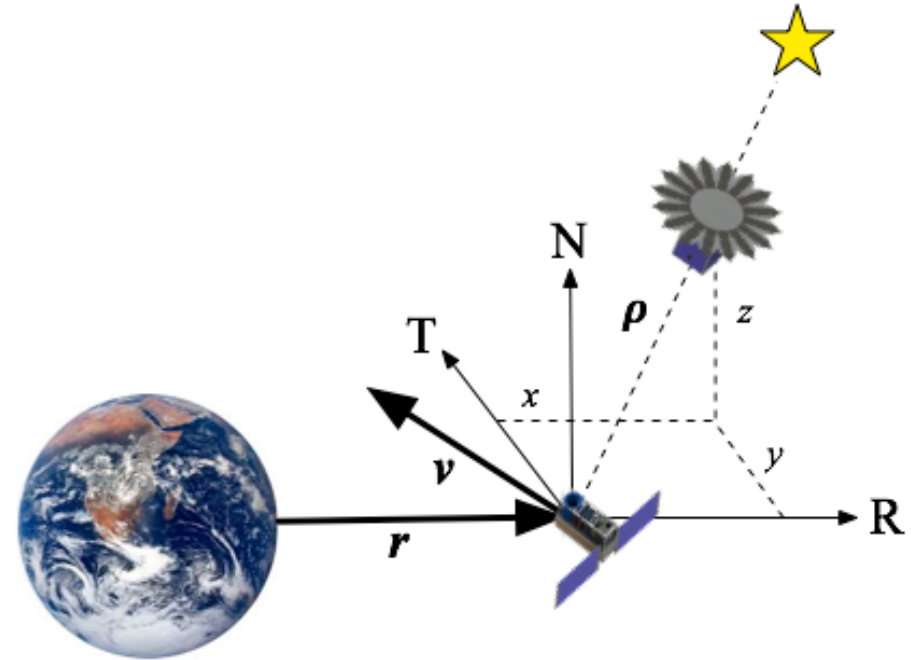
mDOT Operations Concept

- ↗ 2 operations phases
- ↗ Science Phase
 - ↗ Forced motion control to ensure alignment with inertial target
 - ↗ Spacecraft allowed to drift along line-of-sight to save propellant
- ↗ Reconfiguration Phase
 - ↗ Ensure formation is aligned with next target



mDOT Orbit Design

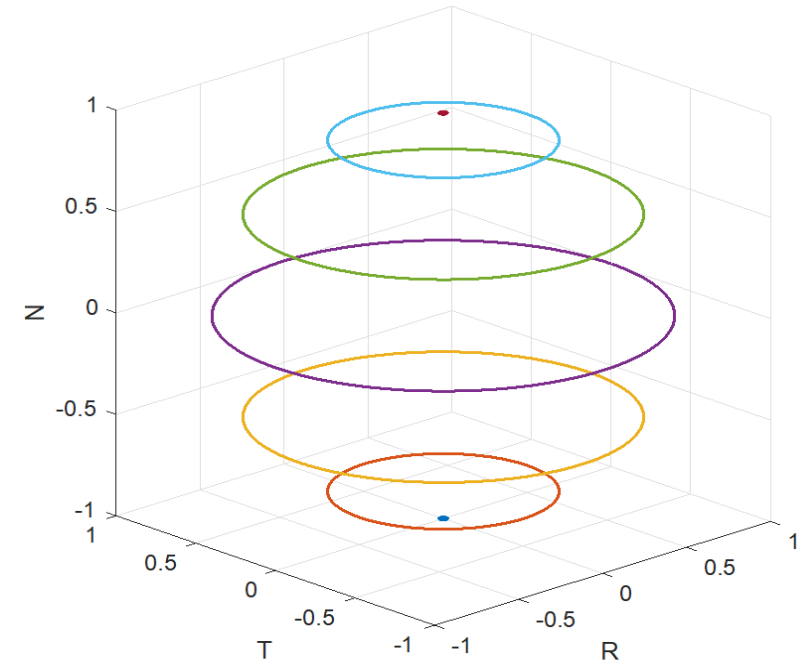
- ↗ Delta-v budget minimized by ensuring relative position and relative acceleration are (anti-)parallel
- ↗ Two options:
 1. Align formation in R direction
 - Requires large difference in semimajor axis -> infeasible
 2. Ensure equal orbit radii



$$\delta \ddot{\mathbf{r}} = \frac{\mu \mathbf{r}_1}{\|\mathbf{r}_1^3\|} - \frac{\mu \mathbf{r}_2}{\|\mathbf{r}_2^3\|}$$

mDOT Orbit Design

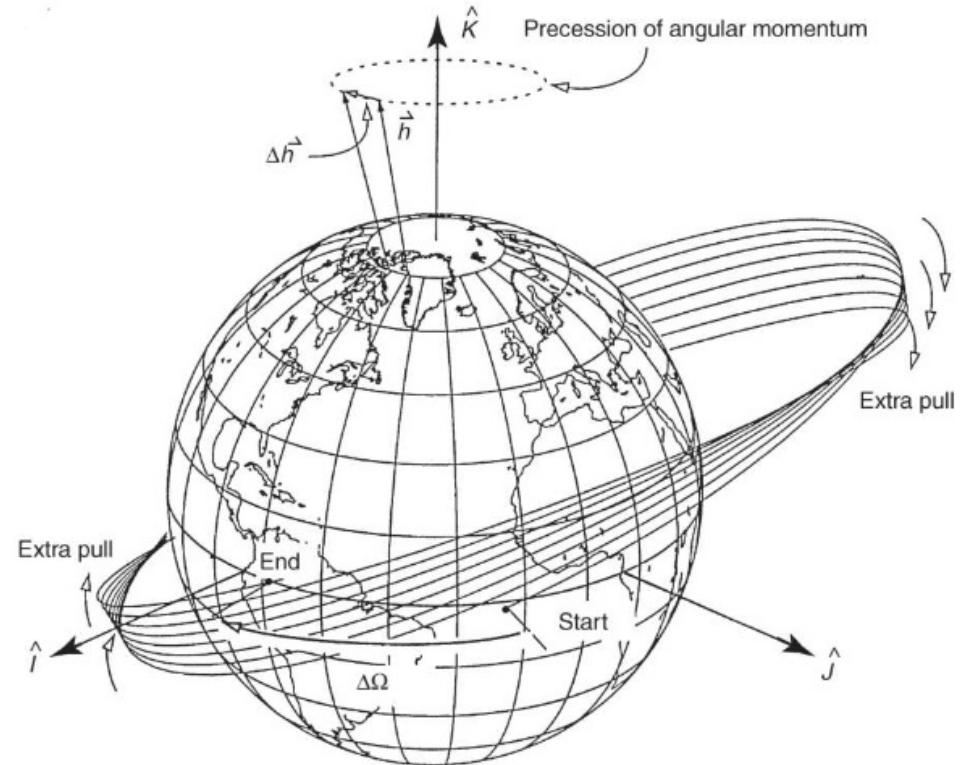
- ↗ Orbit should be selected such that passive trajectory aligns with pointing vector to inertial target to minimize delta-v
- ↗ Trajectory of pointing vector to inertially fixed target is circle in RT-plane with constant offset in N
- ↗ Pointing vector aligned in N direction is stationary
- ↗ **Optimal orbit aligns target with angular momentum vector**



Example paths of pointing vector to inertial target

mDOT: HEO Variant

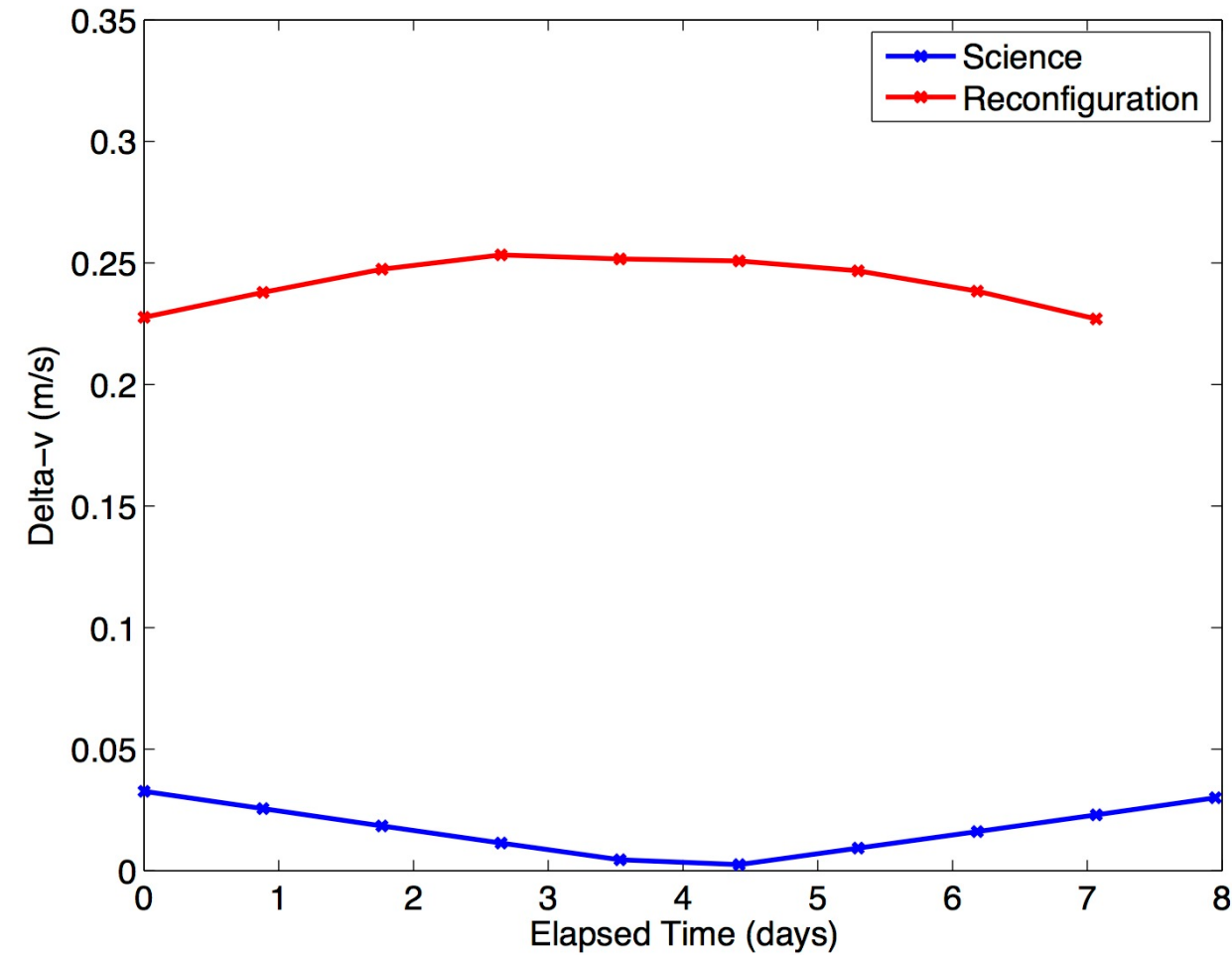
- ↗ Objectives
 - 1. Image Jovian exoplanet
 - 2. Demonstrate 10^{-9} contrast
- ↗ Challenge: J_2 causes the RAAN to precess, changing the angular momentum vector
- ↗ Solution:
 - ↗ Center RAAN at optimal value over mission lifetime
 - ↗ Perform observations at extreme latitudes (ensuring pointing vector evolves in T direction)



mDOT: HEO Variant

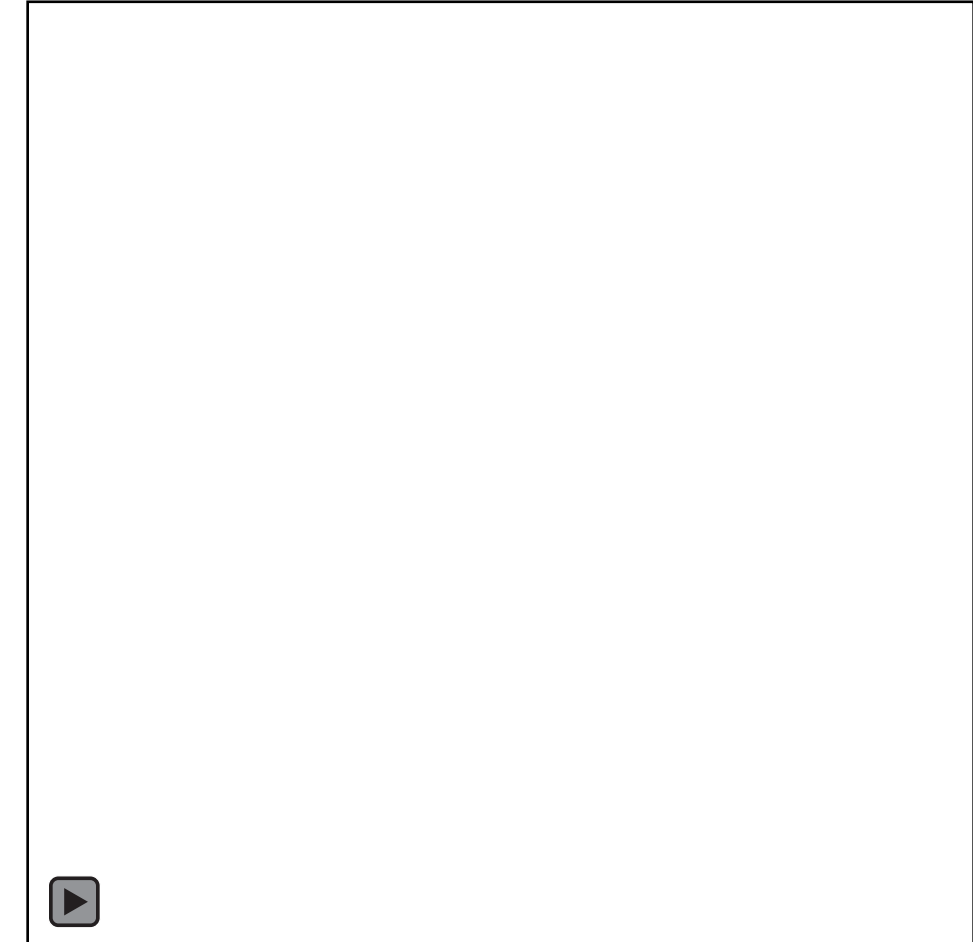
Beta Pictoris Reference Mission

Semi-major axis (km)	30,000
Eccentricity	0.5
Argument of perigee ($^{\circ}$)	45
Inclination ($^{\circ}$)	42
RAAN ($^{\circ}$)	357
Maneuver duration (hr)	1.0
Number of maneuvers	10
Total delta-v cost (m/s)	3.19



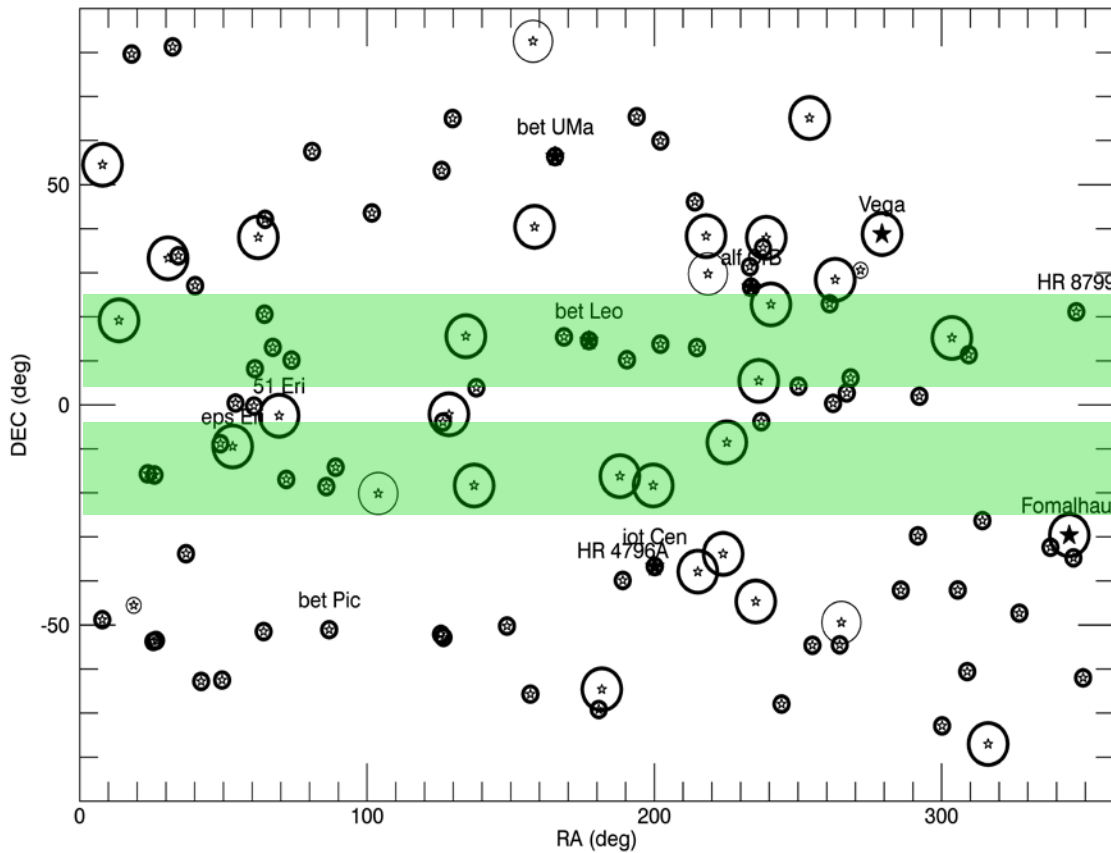
mDOT: LEO Variant

- ↗ Objective: Image multiple exozodii disks at minimum cost
- ↗ Challenge: Large relative accelerations
- ↗ Solution:
 - ↗ Minimize number of science phases needed per target
 - ↗ Exploit J_2 to sweep right ascension



mDOT: LEO Variant

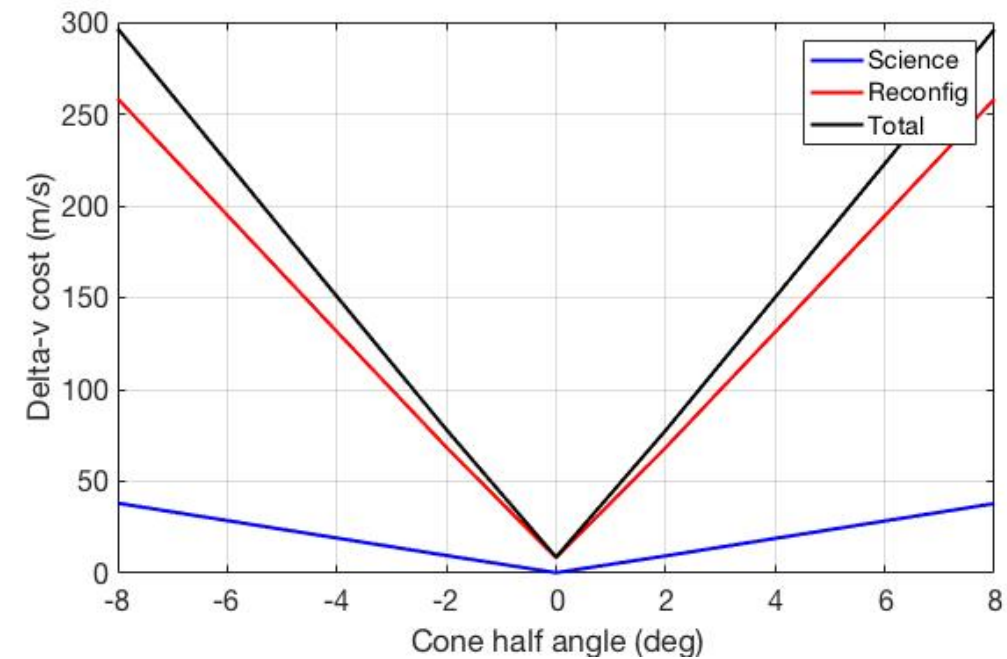
- ↗ How many targets can we see?
 - ↗ 10-20 targets with half angle of several degrees
 - ↗ Depends on range of declinations



Targets that can be imaged from sun-synchronous orbit

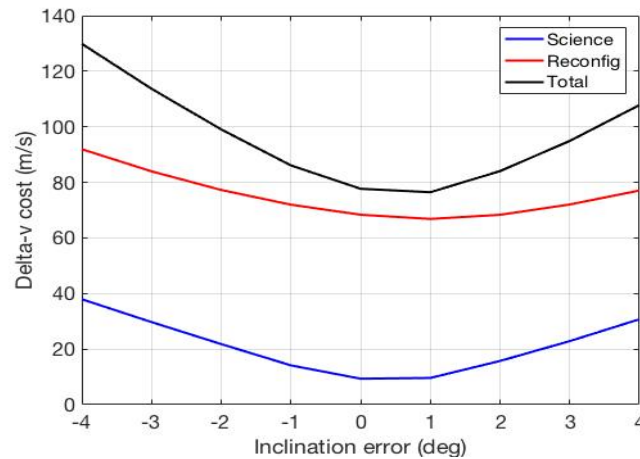
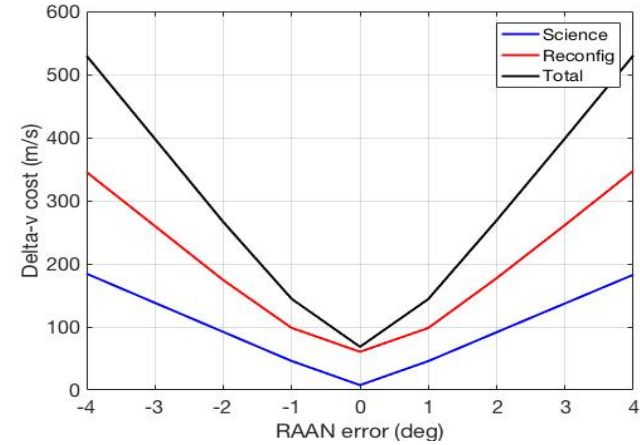
mDOT: LEO Variant

- ↗ How many targets can we see?
 - ↗ 10-20 targets with half angle of several degrees
 - ↗ Depends on range of declinations



mDOT: LEO Variant

- ↗ How does cost vary with errors?
- ↗ Cost is very sensitive to errors in RAAN
 - ↗ RAAN error introduces a radial component to the relative position vector, resulting in a large δa
 - ↗ Sub-degree precision can be ensured through proper timing
- ↗ Cost is insensitive to inclination error
 - ↗ Can tolerate injection errors from launch vehicle



mDOT Orbit & Operations Review

1. Delta-v cost is minimized by aligning angular momentum of orbit with parent star
2. Imaging a Jovian exoplanet around a bright star can be accomplished with reasonable delta-v costs
3. Imaging multiple dust disks is feasible by exploiting passive precession due to J_2 in LEO

mDOT GN&C Requirements

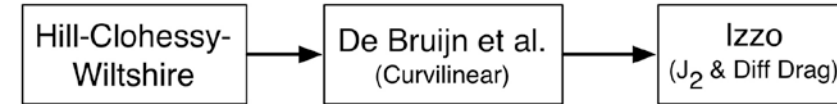
- 1. Accurate dynamics models**
2. Autonomous and efficient maneuver planning

New State Transition Matrices for Perturbed Orbits

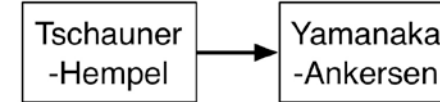
- ↗ Upcoming missions require fast and accurate dynamics models that valid for
 - ↗ Multiple perturbations
 - ↗ Eccentric orbits
- ↗ Use of ROE allows use of astrodynamics tools such as GVE
- ↗ Enabled development of first linear dynamics model including J_2 and drag in eccentric orbits

Relative Position/Velocity

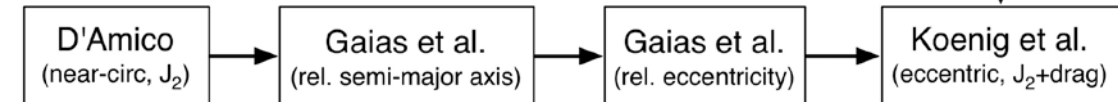
Near-circular



Eccentric



ROE



Derivation Methodology

1. Derive nonlinear EoM from models of perturbations on mean orbits
2. Perform first-order Taylor expansion on EoM
3. Identify state transformation to create LTI system
4. Integrate linear EoM in closed-form

$$\dot{x} = f(x, t)$$

↓ Linearize

$$\dot{x} = A(t)x$$

↓ State transformation

$$y = J(t)x$$

$$\dot{y} = (J(t) + J(t)A(t))J^{-1}(t)y = By$$

↓ Integrate

$$y(t_i + \Delta t) = e^{B\Delta t}y(t_i) = \Phi'(t_i, \Delta t)y(t_i)$$

$$x(t_i + \Delta t) = J^{-1}(t_i + \Delta t)\Phi'(t_i, \Delta t)J(t_i)x(t_i)$$

ROE State Definitions

- ↗ ROE states are defined as explicit functions of the Keplerian orbit elements of the spacecraft
- ↗ Three ROE state definitions included
 - ↗ **Singular:** not unique for circular or equatorial orbits
 - ↗ **Quasi-nonsingular:** not unique for equatorial orbits
 - ↗ **Nonsingular:** always unique
- ↗ Only the quasi-nonsingular state is described for brevity

Singular ROE

$$\delta\boldsymbol{\alpha}_s = \begin{pmatrix} \delta a \\ \delta M \\ \delta e \\ \delta \omega \\ \delta i \\ \delta \Omega \end{pmatrix} = \begin{pmatrix} (a_d - a_c)/a_c \\ M_d - M_c \\ e_d - e_c \\ \omega_d - \omega_c \\ i_d - i_c \\ \Omega_d - \Omega_c \end{pmatrix}$$

Quasi-nonsingular ROE

$$\delta\boldsymbol{\alpha}_{qns} = \begin{pmatrix} \delta a \\ \delta \lambda \\ \delta e_x \\ \delta e_y \\ \delta i_x \\ \delta i_y \end{pmatrix} = \begin{pmatrix} (a_d - a_c)/a_c \\ (M_d + \omega_d) - (M_c + \omega_c) + (\Omega_d - \Omega_c) \cos(i_c) \\ e_d \cos(\omega_d) - e_c \cos(\omega_c) \\ e_d \sin(\omega_d) - e_c \sin(\omega_c) \\ i_d - i_c \\ (\Omega_d - \Omega_c) \sin(i_c) \end{pmatrix}$$

Nonsingular ROE

$$\delta\boldsymbol{\alpha}_{ns} = \begin{pmatrix} \delta a \\ \delta l \\ \delta e_x^* \\ \delta e_y^* \\ \delta i_x^* \\ \delta i_y^* \end{pmatrix} = \begin{pmatrix} (a_d - a_c)/a_c \\ (M_d + \omega_d + \Omega_d) - (M_c + \omega_c + \Omega_c) \\ e_d \cos(\omega_d + \Omega_d) - e_c \cos(\omega_c + \Omega_c) \\ e_d \sin(\omega_d + \Omega_d) - e_c \sin(\omega_c + \Omega_c) \\ \tan(i_d/2) \cos(\Omega_d) - \tan(i_c/2) \cos(\Omega_c) \\ \tan(i_d/2) \sin(\Omega_d) - \tan(i_c/2) \sin(\Omega_c) \end{pmatrix}$$

Case Study: J_2

- ↗ J_2 causes secular drifts in
 - ↗ RAAN (Ω)
 - ↗ Argument of perigee (ω)
 - ↗ Mean anomaly (M)
- ↗ Secular drifts depend on
 - ↗ Semi-major axis (a)
 - ↗ Eccentricity (e, η)
 - ↗ Inclination (i)
- ↗ Resulting plant matrix is time-varying and periodic
 - ↗ Due to precession of ω , which affects e_x and e_y

$$\begin{pmatrix} \dot{M} \\ \dot{\omega} \\ \dot{\Omega} \end{pmatrix} = \frac{3}{4} \frac{J_2 R_E^2 \sqrt{\mu}}{a^{7/2} \eta^4} \begin{pmatrix} \eta(3 \cos^2(i) - 1) \\ 5 \cos^2(i) - 1 \\ -2 \cos(i) \end{pmatrix}$$

Secular drifts due to J_2 (Brouwer 1959)

$$A^{J_2}(t) = \kappa \begin{bmatrix} 0 & 0 & 0 & 0 & 0 & 0 \\ -\frac{7}{2}EP - \frac{3n}{2\kappa} & 0 & e_x GFP & e_y GFP & -FS & 0 \\ \frac{7}{2}e_y Q & 0 & -4e_x e_y GQ & -(1 + 4e_y^2)GQ & 5e_y S & 0 \\ -\frac{7}{2}e_x Q & 0 & (1 + 4e_x^2)GQ & 4e_x e_y GQ & -5e_x S & 0 \\ 0 & 0 & 0 & 0 & 0 & 0 \\ \frac{7}{2}S & 0 & -4e_x GS & -4e_y GS & 2T & 0 \end{bmatrix}$$

Time-varying plant matrix

Case Study: J₂

- ↗ Coordinate transformation is a simple rotation of the relative eccentricity vector
- ↗ Modified plant matrix is a function of only a, e , and i
- ↗ Structure of modified matrix admits trivial solution
- ↗ Coordinate transformations required at beginning and end of propagation

$$\mathbf{J}_{qns}(\alpha_c) = \begin{bmatrix} \mathbf{I}^{2 \times 2} & \mathbf{0}^{2 \times 2} & \mathbf{0}^{2 \times 2} \\ \mathbf{0}^{2 \times 2} & \cos(\omega) & \sin(\omega) \\ \mathbf{0}^{2 \times 2} & -\sin(\omega) & \cos(\omega) \\ \mathbf{0}^{2 \times 2} & \mathbf{0}^{2 \times 2} & \mathbf{I}^{2 \times 2} \end{bmatrix}$$

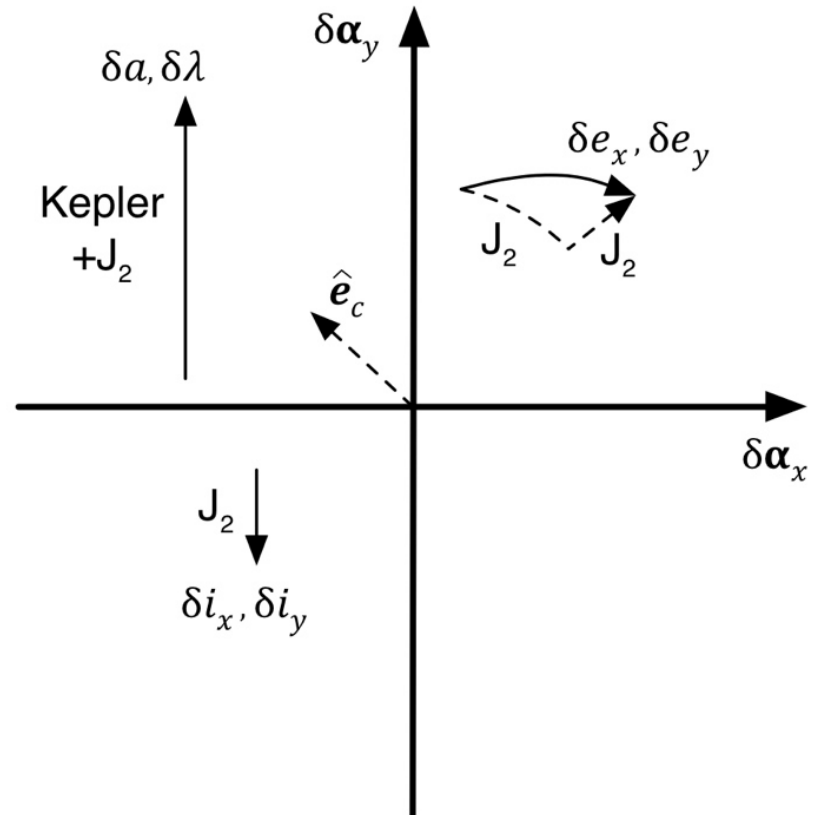
Linear state transformation

$$\mathbf{A}'(\alpha_c(t)) = \kappa \begin{bmatrix} 0 & 0 & 0 & 0 & 0 & 0 \\ -\frac{3}{2} \frac{n}{\kappa} - \frac{7}{2} EP & 0 & eFGP & 0 & -FS & 0 \\ 0 & 0 & 0 & 0 & 0 & 0 \\ -\frac{7}{2} eQ & 0 & 4e^2 GQ & 0 & -5eS & 0 \\ 0 & 0 & 0 & 0 & 0 & 0 \\ \frac{7}{2} S & 0 & -4eGS & 0 & 2T & 0 \end{bmatrix}$$

Modified plant matrix

Case Study: J_2

- ↗ J_2 and Kepler produce four effects on the quasi-nonsingular ROE
 - ↗ Linear drift of $\delta\lambda$
 - ↗ Rotation of δe
 - ↗ Linear drift of δe perpendicular to e
 - ↗ Linear drift of δi_y
- ↗ Along track separation is modeled differently from Gim-Alfriend
 - ↗ Differences caused by use of mean anomaly instead of true anomaly



Case Study: $J_2 + \text{Drag}$

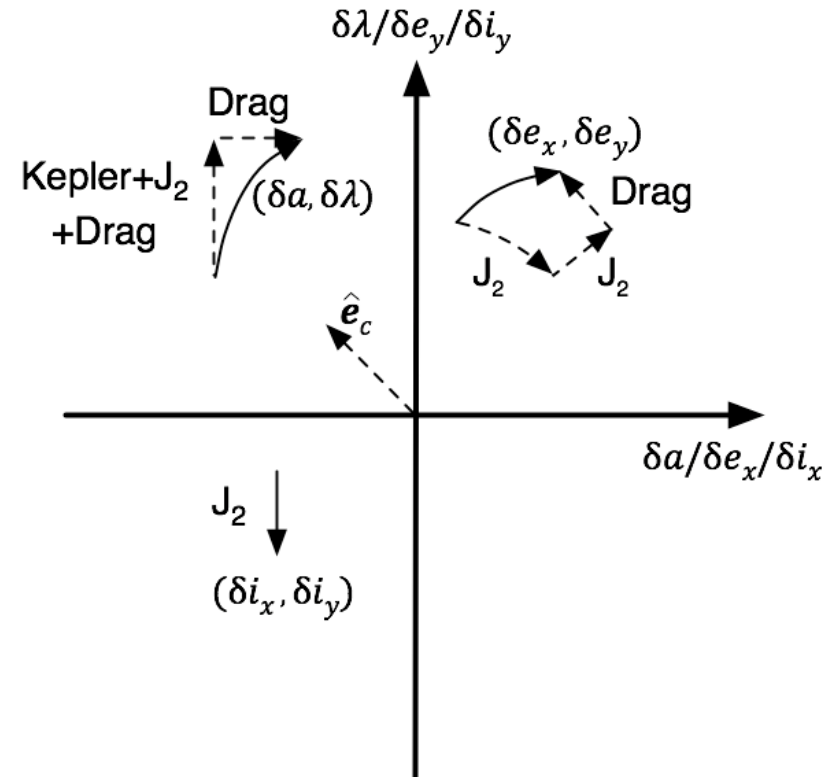
- ↗ Uncertainty in density model is captured in state definition
- ↗ State is augmented with three time derivatives **only due to differential drag**
- ↗ Plant matrix can be simplified for eccentric orbits
 - ↗ Relationship between time derivatives of δa and $\delta e'_x$ governed by circularization constraint

$$\begin{pmatrix} \dot{\delta\alpha}' \\ \ddot{\delta a}_{drag} \\ \ddot{\delta e}'_{x,drag} \\ \ddot{\delta e}'_{y,drag} \end{pmatrix} = \begin{bmatrix} 0 & 0 & 0 & 0 & 0 & 0 & 1 & 0 & 0 \\ X & 0 & X & 0 & X & 0 & 0 & 0 & 0 \\ 0 & 0 & 0 & 0 & 0 & 0 & 0 & 1 & 0 \\ X & 0 & X & 0 & X & 0 & 0 & 0 & 1 \\ 0 & 0 & 0 & 0 & 0 & 0 & 0 & 0 & 0 \\ X & 0 & X & 0 & X & 0 & 0 & 0 & 0 \\ 0 & 0 & 0 & 0 & 0 & 0 & 0 & 0 & 0 \\ 0 & 0 & 0 & 0 & 0 & 0 & 0 & 0 & 0 \\ 0 & 0 & 0 & 0 & 0 & 0 & 0 & 0 & 0 \end{bmatrix} \begin{pmatrix} \delta\alpha' \\ \delta a_{drag} \\ \delta e'_{x,drag} \\ \delta e'_{y,drag} \end{pmatrix}$$

Density-model-free plant matrix

Case Study: J_2 + Drag

- ↗ Differential drag introduces three new effects in eccentric orbits
 - ↗ Linear drift of δa
 - ↗ Quadratic drift of $\delta \lambda$
 - ↗ Linear drift of δe parallel to e
- ↗ Quadratic couplings between drag and J_2 are small



Combined effects of J_2 and differential drag on ROE in eccentric orbits

Validation: Scenario Definition

- ↗ Three test cases selected to cover range of past and future missions
- ↗ Test 1
 - ↗ Near-circular LEO
 - ↗ Small Separation
- ↗ Test 2
 - ↗ Small eccentricity
 - ↗ Moderate separation
 - ↗ Near equatorial
- ↗ Test 3
 - ↗ Large eccentricity
 - ↗ Large cross-track separation
- ↗ All test cases propagated for 10 orbits

Chief orbit (unit)	Test Case 1	Test Case 2	Test Case 3
Initial date	Jan 1, 2002	Jan 1, 2002	Jan 1, 2002
Initial time	00:00:00	00:00:00	00:00:00
a (km)	6,917	8,348	13,256
e	0.02	0.2	0.5
i ($^{\circ}$)	30	1	70
Ω ($^{\circ}$)	60	120	180
ω ($^{\circ}$)	180	120	60
M ($^{\circ}$)	180	180	180
h_p (km)	400	300	250

Relative state (unit)	Test Case 1	Test Case 2	Test Case 3
$a\delta a$ (m)	0	25	100
$a\delta\lambda$ (m)	0	4,000	5,000
$a\delta e_x$ (m)	200	-1,000	5,000
$a\delta e_y$ (m)	-200	1,000	5,000
$a\delta i_x$ (m)	200	1,000	-5,000
$a\delta i_y$ (m)	-200	0	20,000
δB	0.4	0.2	0.1

Mass	Cross-section area	Drag Coefficient	Reflectance Coefficient
100 kg	1 m ²	1	1

Test case parameters

Validation: Results

STM	Test	Harris-Priester Atmosphere						Jacchia-Gill Atmosphere					
		$\epsilon_{\delta a}$ (m)	$\epsilon_{\delta \lambda}$ (m)	$\epsilon_{\delta e_x}$ (m)	$\epsilon_{\delta e_y}$ (m)	$\epsilon_{\delta i_x}$ (m)	$\epsilon_{\delta i_y}$ (m)	$\epsilon_{\delta a}$ (m)	$\epsilon_{\delta \lambda}$ (m)	$\epsilon_{\delta e_x}$ (m)	$\epsilon_{\delta e_y}$ (m)	$\epsilon_{\delta i_x}$ (m)	$\epsilon_{\delta i_y}$ (m)
J_2	1	38.5	1808.8	13.5	11.3	0.9	2.5	71.0	3417.0	22.1	17.1	1.0	4.9
	2	37.1	1828.0	25.6	18.7	0.3	1.2	52.2	2455.3	25.6	34.3	0.7	1.2
	3	148.7	7146.1	64.8	34.1	1.5	4.6	211.3	9966.5	90.4	51.6	1.2	6.3
DMS	1	17.9	832.4	6.8	7.7	0.9	1.2	50.3	2439.7	2.2	13.5	1.0	3.5
	2	5.9	278.9	10.3	5.7	0.6	1.1	11.0	509.3	8.9	9.2	0.7	1.2
	3	45.2	1986.8	18.4	15.3	1.5	2.7	17.6	833.6	7.3	3.7	1.2	3.0
DMF-E	1	0.4	25.9	24.6	4.6	0.9	0.2	1.9	83.0	47.0	5.0	1.0	0.2
	2	0.6	24.6	9.5	6.9	0.6	1.1	1.3	67.5	10.2	6.5	0.7	1.2
	3	2.9	202.2	2.1	3.6	1.5	2.6	9.5	343.5	4.5	5.4	1.6	3.3
DMF-A	1	0.4	26	0.4	0.4	0.9	0.2	1.9	82.9	1.7	1.0	1.0	0.2
	2	0.6	24.6	8.3	5.7	0.6	1.1	1.3	67.4	8.9	5.2	0.7	1.2
	3	2.9	202.2	2.9	0.9	1.5	2.6	9.5	346.6	2.2	5.7	2.0	1.2

Validation: Results

STM	Test	Harris-Priester Atmosphere						Jacchia-Gill Atmosphere					
		$\epsilon_{\delta a}$ (m)	$\epsilon_{\delta \lambda}$ (m)	$\epsilon_{\delta e_x}$ (m)	$\epsilon_{\delta e_y}$ (m)	$\epsilon_{\delta i_x}$ (m)	$\epsilon_{\delta i_y}$ (m)	$\epsilon_{\delta a}$ (m)	$\epsilon_{\delta \lambda}$ (m)	$\epsilon_{\delta e_x}$ (m)	$\epsilon_{\delta e_y}$ (m)	$\epsilon_{\delta i_x}$ (m)	$\epsilon_{\delta i_y}$ (m)
J_2	1	38.5	1808.8	13.5	11.3	0.9	2.5	71.0	3417.0	22.1	17.1	1.0	4.9
	2	37.1	1828.0	25.6	18.7	0.3	1.2	52.2	2455.3	25.6	34.3	0.7	1.2
	3	148.7	7146.1	64.8	34.1	1.5	4.6	211.3	9966.5	90.4	51.6	1.2	6.3
DMS	1	17.9	832.4	4.8	7.7	0.9	1.2	50.3	299.7	2.2	13.5	1.0	3.5
	2	5.9	278.9	10.3	5.7	0.6	1.1	11.0	509.3	8.9	9.2	0.7	1.2
	3	45.2	1986.8							3.6	7.3	3.7	1.2
DMF-E	1	0.4	25.9							0	47.0	5.0	1.0
	2	0.6	24.6							5	10.2	6.5	0.7
	3	2.9	202.2	2.1	3.6	1.5	2.6	9.5	343.5	4.5	5.4	1.6	3.3
DMF-A	1	0.4	26	0.4	0.4	0.9	0.2	1.9	82.9	1.7	1.0	1.0	0.2
	2	0.6	24.6	8.3	5.7	0.6	1.1	1.3	67.4	8.9	5.2	0.7	1.2
	3	2.9	202.2	2.9	0.9	1.5	2.6	9.5	346.6	2.2	5.7	2.0	1.2

In-plane errors due to
unmodeled differential drag

Validation: Results

STM	Test	Harris-Priester Atmosphere						Jacchia-Gill Atmosphere					
		$\epsilon_{\delta a}$ (m)	$\epsilon_{\delta \lambda}$ (m)	$\epsilon_{\delta e_x}$ (m)	$\epsilon_{\delta e_y}$ (m)	$\epsilon_{\delta i_x}$ (m)	$\epsilon_{\delta i_y}$ (m)	$\epsilon_{\delta a}$ (m)	$\epsilon_{\delta \lambda}$ (m)	$\epsilon_{\delta e_x}$ (m)	$\epsilon_{\delta e_y}$ (m)	$\epsilon_{\delta i_x}$ (m)	$\epsilon_{\delta i_y}$ (m)
J_2	1	38.5	1808.8	13.5	11.3	0.9	2.5	71.0	3417.0	22.1	17.1	1.0	4.9
	2	37.1	1828.0	Dramatic improvement for STMs using density-model-free drag						25.6	34.3	0.7	1.2
	3	148.7	7146.1							90.4	51.6	1.2	6.3
DMS	1	17.9	832.4	6.8	7.7	0.9	1.2	58.3	2439.7	2.2	13.5	1.0	3.5
	2	5.9	278.9	10.3	5.7	0.6	1.1	11.0	509.3	8.9	9.2	0.7	1.2
	3	45.2	1986.8	3.4	15.3	1.5	2.7	17.6	833.1	7.3	3.7	1.2	3.0
DMF-E	1	0.4	25.9	24.6	4.6	0.9	0.2	1.9	83.0	47.0	5.0	1.0	0.2
	2	0.6	24.6	9.5	6.9	0.6	1.1	1.3	67.5	10.2	6.5	0.7	1.2
	3	2.9	202.2	2.1	3.6	1.5	2.6	9.5	343.5	4.5	5.4	1.6	3.3
DMF-A	1	0.4	26	0.4	0.4	0.9	0.2	1.9	82.9	1.7	1.0	1.0	0.2
	2	0.6	24.6	8.3	5.7	0.6	1.1	1.3	67.4	8.9	5.2	0.7	1.2
	3	2.9	202.2	2.9	0.9	1.5	2.6	9.5	346.6	2.2	5.7	2.0	1.2

Validation: Results

STM	Test	Harris-Priester Atmosphere						Jacchia-Gill Atmosphere					
		$\epsilon_{\delta a}$ (m)	$\epsilon_{\delta \lambda}$ (m)	$\epsilon_{\delta e_x}$ (m)	$\epsilon_{\delta e_y}$ (m)	$\epsilon_{\delta i_x}$ (m)	$\epsilon_{\delta i_y}$ (m)	$\epsilon_{\delta a}$ (m)	$\epsilon_{\delta \lambda}$ (m)	$\epsilon_{\delta e_x}$ (m)	$\epsilon_{\delta e_y}$ (m)	$\epsilon_{\delta i_x}$ (m)	$\epsilon_{\delta i_y}$ (m)
	1	38.5	1808.8	13.5	11.3	0.9	2.5	71.0	3417.0	22.1	17.1	1.0	4.9
J_2	2	37.1	1828.0	Remaining relative eccentricity error due to invalid circularization assumption						3	0.7	1.2	
	3	148.7	7146.1							6	1.2	6.3	
	1	17.9	832.4	6.8	7.1	0.9	1.2	50.3	2439.7	2.2	13.5	1.0	3.5
DMS	2	5.9	278.9	10.3	5.7	0.6	1.1	11.0	509.3	3.9	9.2	0.7	1.2
	3	45.2	1986.8	18.4	15.3	1.5	2.7	17.6	833.6	7.1	3.7	1.2	3.0
	1	0.4	25.9	24.6	4.6	0.9	0.2	1.9	83.0	47.0	5.0	1.0	0.2
DMF-E	2	0.6	24.6	9.5	6.9	0.6	1.1	1.3	67.5	10.2	6.5	0.7	1.2
	3	2.9	202.2	2.1	3.6	1.5	2.6	9.5	343.5	4.5	5.4	1.6	3.3
	1	0.4	26	0.4	0.4	0.9	0.2	1.9	82.9	1.7	1.0	1.0	0.2
DMF-A	2	0.6	24.6	8.3	5.7	0.6	1.1	1.3	67.4	8.9	5.2	0.7	1.2
	3	2.9	202.2	2.9	0.9	1.5	2.6	9.5	346.6	2.2	5.7	2.0	1.2

Validation: Results

STM	Test	Harris-Priester Atmosphere						Jacchia-Gill Atmosphere					
		$\epsilon_{\delta a}$ (m)	$\epsilon_{\delta \lambda}$ (m)	$\epsilon_{\delta e_x}$ (m)	$\epsilon_{\delta e_y}$ (m)	$\epsilon_{\delta i_x}$ (m)	$\epsilon_{\delta i_y}$ (m)	$\epsilon_{\delta a}$ (m)	$\epsilon_{\delta \lambda}$ (m)	$\epsilon_{\delta e_x}$ (m)	$\epsilon_{\delta e_y}$ (m)	$\epsilon_{\delta i_x}$ (m)	$\epsilon_{\delta i_y}$ (m)
J_2	1	38.5	1808.8	13.5	11.3	0.9	2.5	71.0	3417.0	22.1	17.1	1.0	4.9
	2	37.1	1828.0	25.6	18.7	0.3	1.2	52.2	2455.3	25.6	34.3	0.7	1.2
	3	148.7	7146.1	64	No significant accuracy loss for simplified STM in eccentric orbits						51.6	1.2	6.3
DMS	1	17.9	832.4	6							13.5	1.0	3.5
	2	5.9	278.9	10.5	5.7	0.0	1.1	11.0	309.5	8.9	9.2	0.7	1.2
	3	45.2	1986.8	18.4	15.3	1.5	2.7	17.6	833.6	7.3	3.7	1.2	3.0
DMF-E	1	0.4	25.9	24.6	4.6	0.9	0.2	1.9	83.0	47.0	5.0	1.0	0.2
	2	0.6	24.6	9.5	6.9	0.6	1.1	1.3	67.5	10.2	6.5	0.7	1.2
	3	2.9	202.2	2.1	3.6	1.5	2.6	9.5	343.5	4.5	5.4	1.6	3.3
DMF-A	1	0.4	26	0.4	0.4	0.9	0.2	1.9	82.9	1.7	1.0	1.0	0.2
	2	0.6	24.6	8.3	5.7	0.6	1.1	1.3	67.4	8.9	5.2	0.7	1.2
	3	2.9	202.2	2.9	0.9	1.5	2.6	9.5	346.6	2.2	5.7	2.0	1.2

State Transition Matrix Review

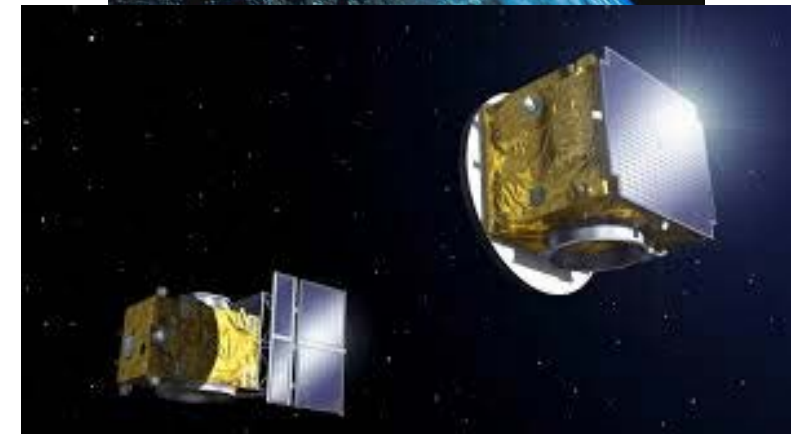
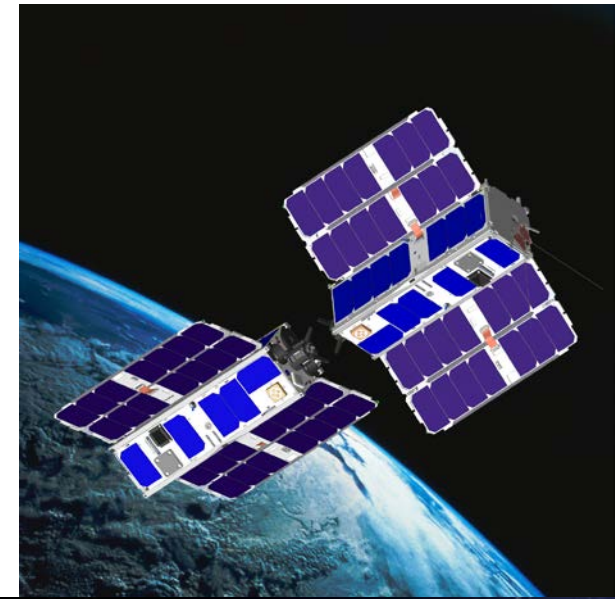
1. Developed simple derivation methodology that accommodates multiple state definitions
2. Derived STMs that include effects of both J_2 and differential drag on mean ROE
3. Validated models against high-fidelity simulations

mDOT GN&C Requirements

1. Accurate dynamics models
2. **Autonomous and efficient maneuver planning**

Globally Optimal Impulsive Control of LTV Systems

- ↗ Proposed formation flying missions require more efficient control algorithms for challenging scenarios
- ↗ Lifetimes are limited by propellant capacity
- ↗ Missions must operate in eccentric orbits with multiple perturbations
- ↗ Multiple attitude modes result in time-varying cost of a specified maneuver



Problem Statement

- ↗ Develop a solution methodology that provides globally optimal impulsive control inputs for fixed-time, fixed-end-condition control of linear time-varying systems
- ↗ Solution based on geometric relationships between reachable sets
- ↗ Resulting algorithm accommodates:
 - ↗ Multiple state definitions
 - ↗ Multiple perturbations in eccentric orbits
 - ↗ No-control windows
 - ↗ A wide range of **time-varying cost functions**

Problem Formulation

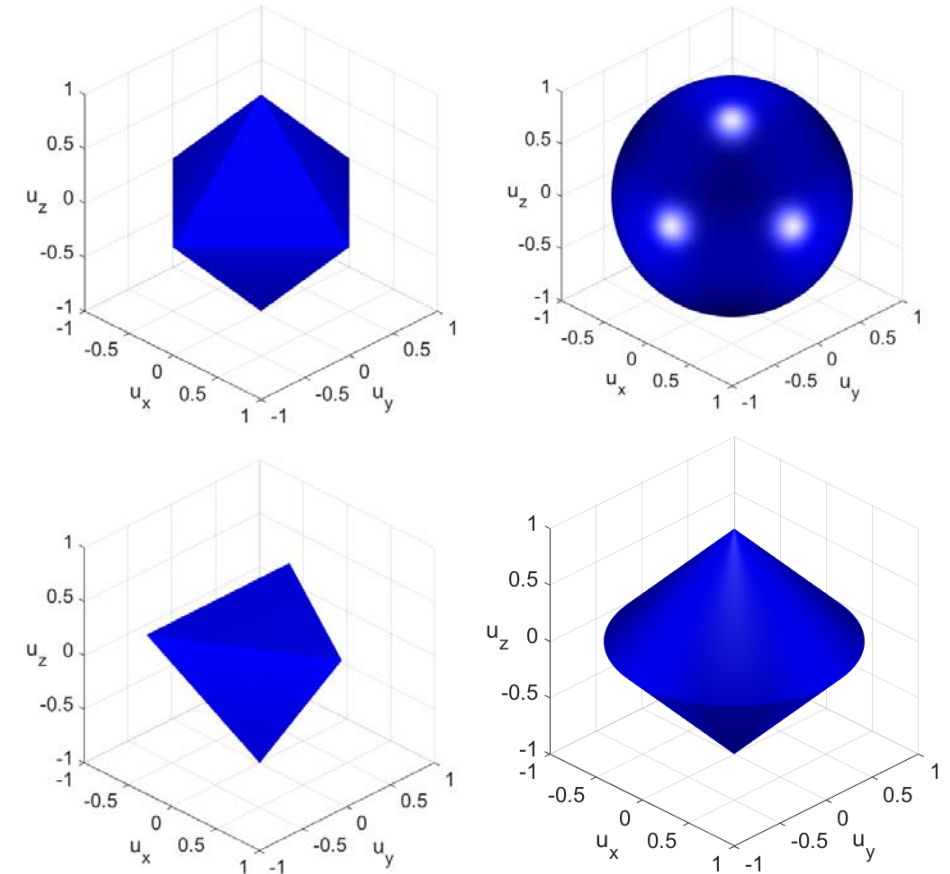
$$\text{Minimize: } \sum f(\mathbf{u}_j, t) \quad \text{Subject to: } \mathbf{x}(t_f) = \boldsymbol{\Phi}(t_i, t_f)\mathbf{x}(t_i) + \sum \boldsymbol{\Phi}(t_j, t_f)\mathbf{B}(t_j)\mathbf{u}_j$$
$$t_j \in T \quad T \subseteq [t_i, t_f]$$

$$\text{Definition: } \mathbf{x}_{des} = \mathbf{x}(t_f) - \boldsymbol{\Phi}(t_i, t_f)\mathbf{x}(t_i) \quad \boldsymbol{\Gamma}(t_j) = \boldsymbol{\Phi}(t_j, t_f)\mathbf{B}(t_j)\mathbf{u}_j$$

$$\text{Minimize: } \sum f(\mathbf{u}_j, t) \quad \text{Subject to: } \mathbf{x}_{des} = \sum \boldsymbol{\Gamma}(t_j)\mathbf{u}_j$$
$$t_j \in T \quad T \subseteq [t_i, t_f]$$

Cost of Control Input

- ↗ Propellant cost of a maneuver is:
 - 1) Linear in magnitude
 - 2) Varies with direction
- ↗ Cost of control input at any specified time must be norm-like:
 - 1) Cost proportional to $\|\mathbf{u}\|$
 - 2) Sublevel sets are convex

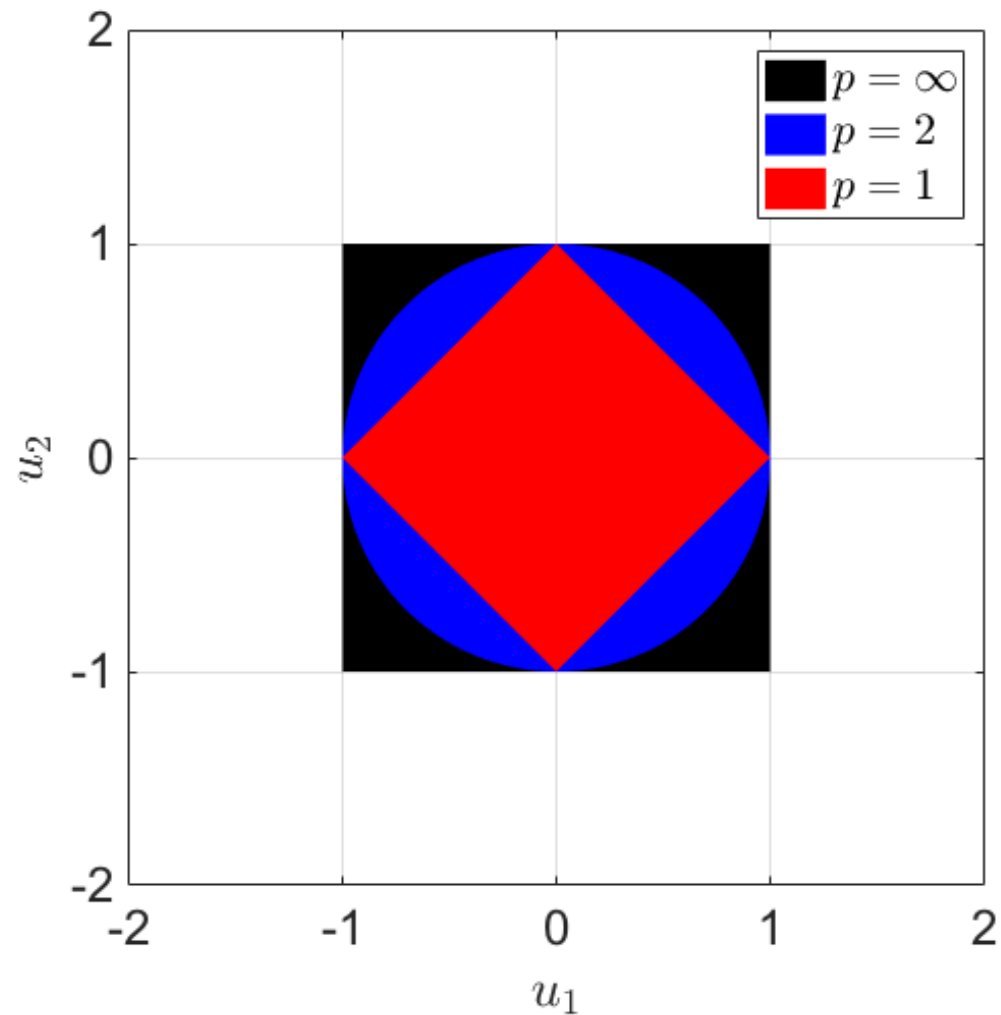


Example cost function sublevel sets

Set Definitions

- ↗ $U(c, t)$: The set of control actions with a cost no larger than c at a time t

$$U(c, t) = \{\mathbf{u} : f(\mathbf{u}, t) \leq c\}$$



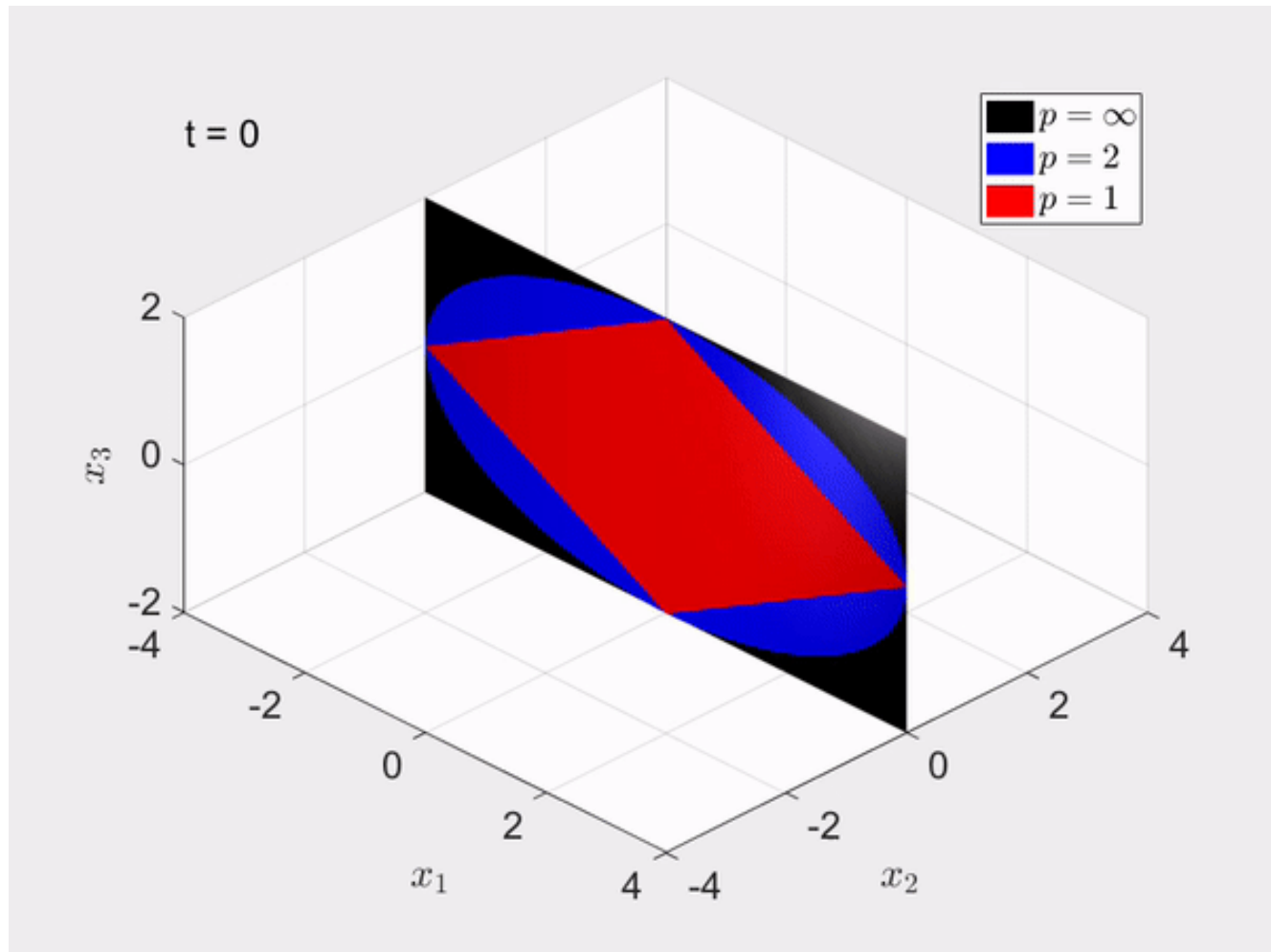
Set Definitions

- ↗ $S(c, t)$: The set of reachable states from a single control action of cost c executed at time t

$$S(c, t) = \{y : y = \Gamma(t)u, u \in U(c, t)\}$$

- ↗ Cost of reaching any y is proportional to its magnitude
- ↗ Example System:

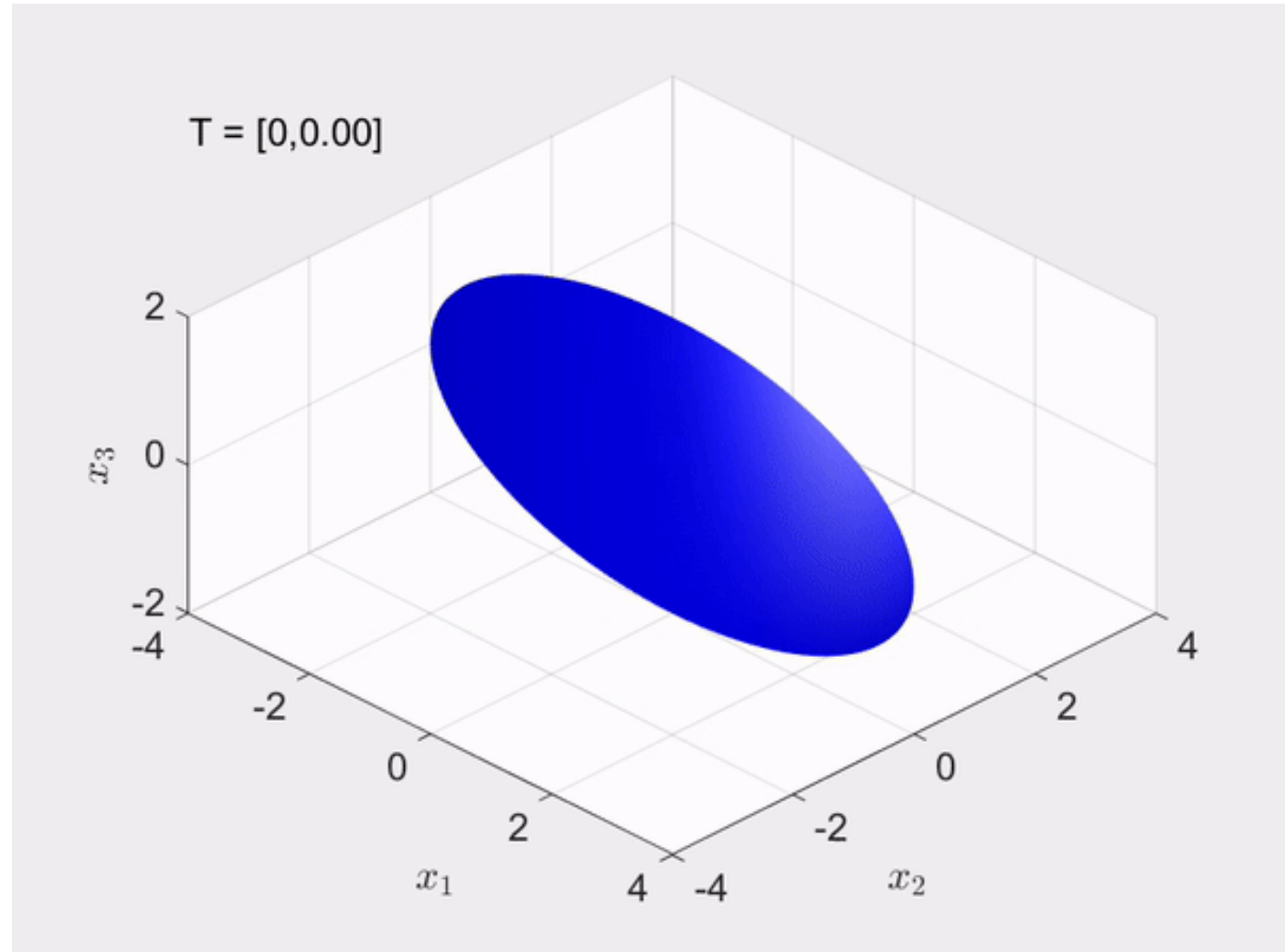
$$\Gamma(t) = 0.5 \begin{bmatrix} (5 + 3\cos(4t))\cos(t) & 0 \\ (5 + 3\cos(4t))\sin(t) & 0 \\ 0 & 3 + \cos(4t) \end{bmatrix}$$



Set Definitions

- ↗ $S(c)$: The set of reachable states from a single control action of cost c executed at any time t in T

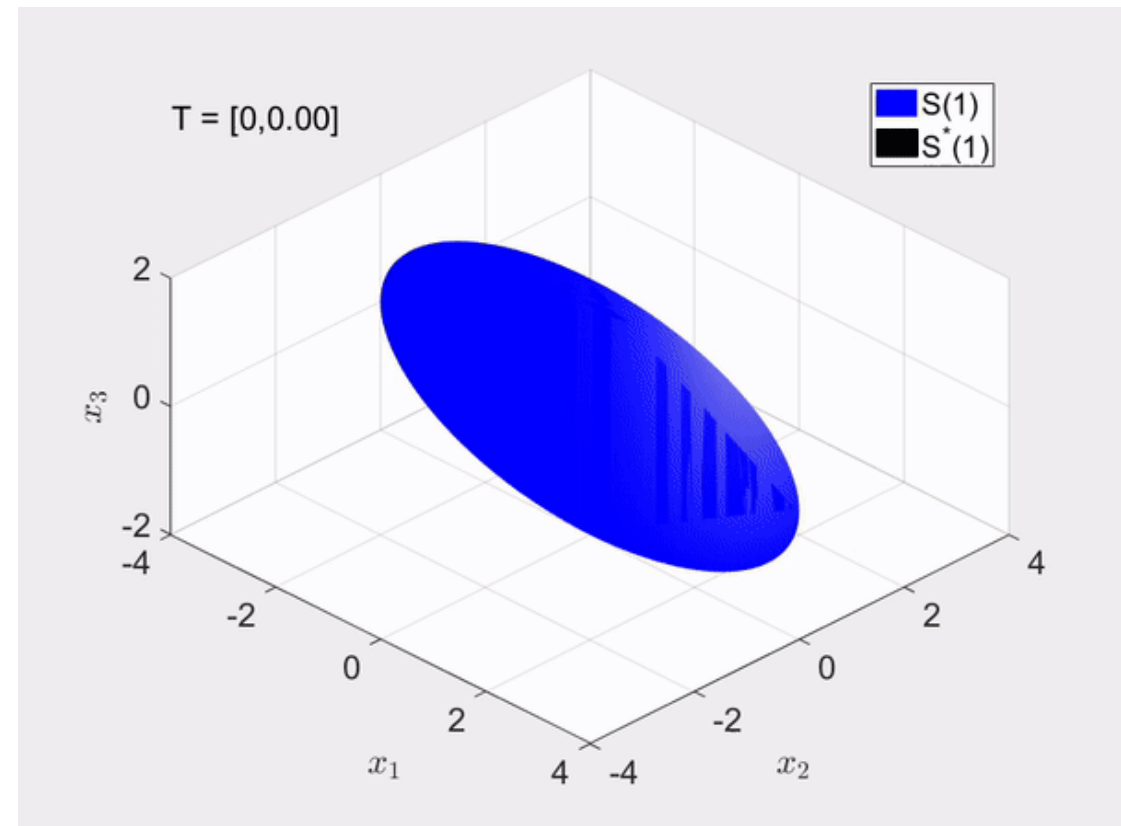
$$S(c) = \bigcup_{t \in T} S(c, t)$$



Set Definitions

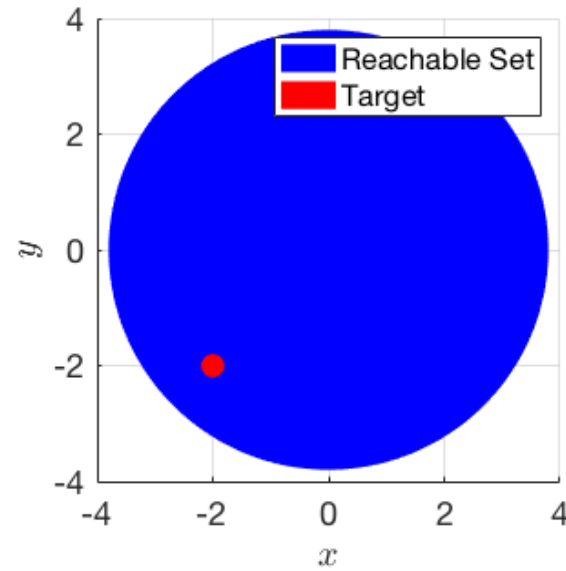
- ↗ $S^*(c)$: The set of reachable states from an arbitrary number of control actions with a total cost of c executed at times in T
- ↗ $S^*(c)$ is the convex hull of $S(c)$
- ↗ All points in the boundary of $S^*(c)$ lie in a polytope of points in $S(c)$ with n vertices
- ↗ **There must exist an optimal control input sequence consisting of no more than n impulses**

$$S^*(c) = \left\{ \mathbf{y} : \mathbf{y} = \sum \Gamma(t_j) \mathbf{u}_j, \mathbf{u}_j \in U(c_j), t_j \in T, \sum c_j \leq c \right\}$$

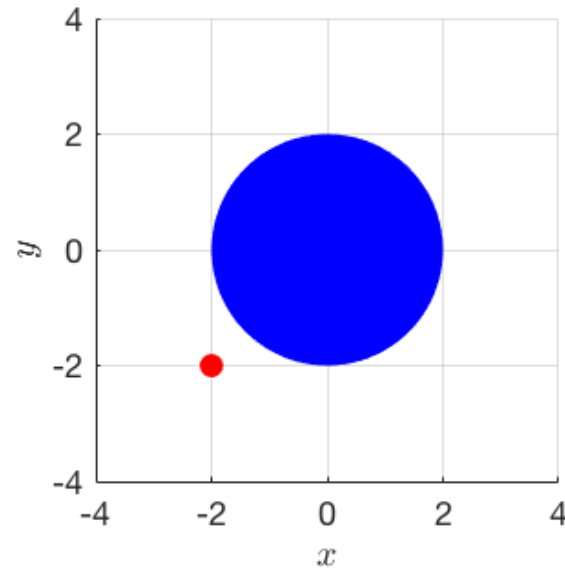


Optimality Condition

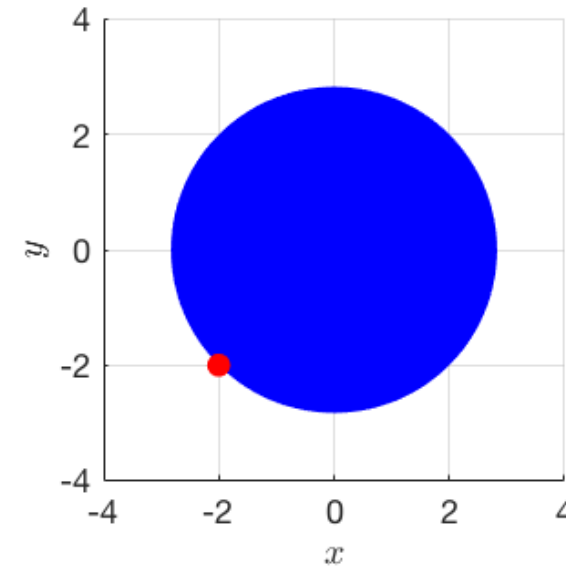
- ↗ A cost is optimal if the target state is on the boundary of the reachable set



Suboptimal cost



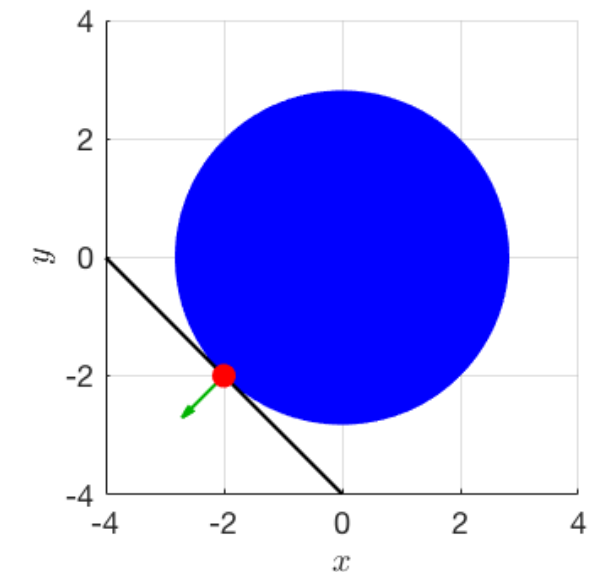
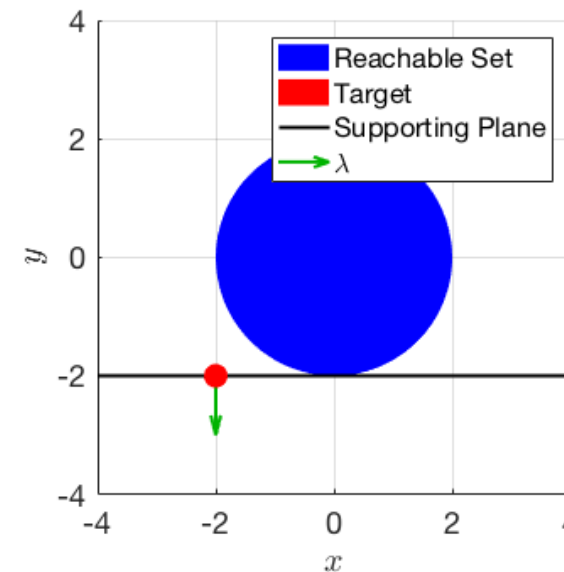
Infeasible cost



Optimal cost

Solution Methodology: Primal/Dual Problems

- ↗ Primal problem: minimize cost subject to constraint that target is reachable
 - ↗ Shape of reachable set not known in advance
- ↗ Dual problem: maximize cost subject to constraint that target cannot be reached at a lesser cost
 - ↗ **Equivalent to maximizing the cost to reach a plane that contains the target state**



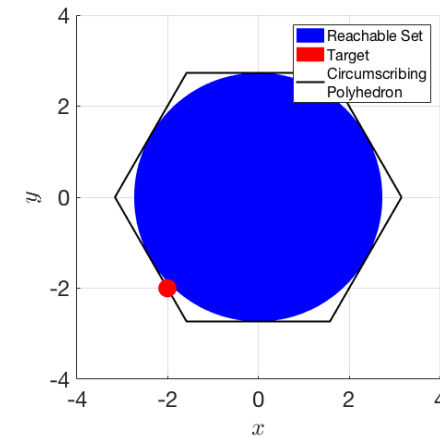
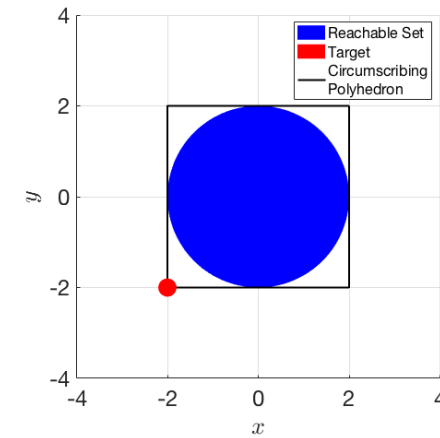
Example supporting hyperplanes

Lower Bounds on Minimum Cost

- Each λ provides a lower bound on the minimum cost:

$$\Delta v_{lb} = \frac{\lambda^T x_{des}}{\max_{t \in T, u \in U(1,t)} \lambda^T \Gamma(t) u}$$

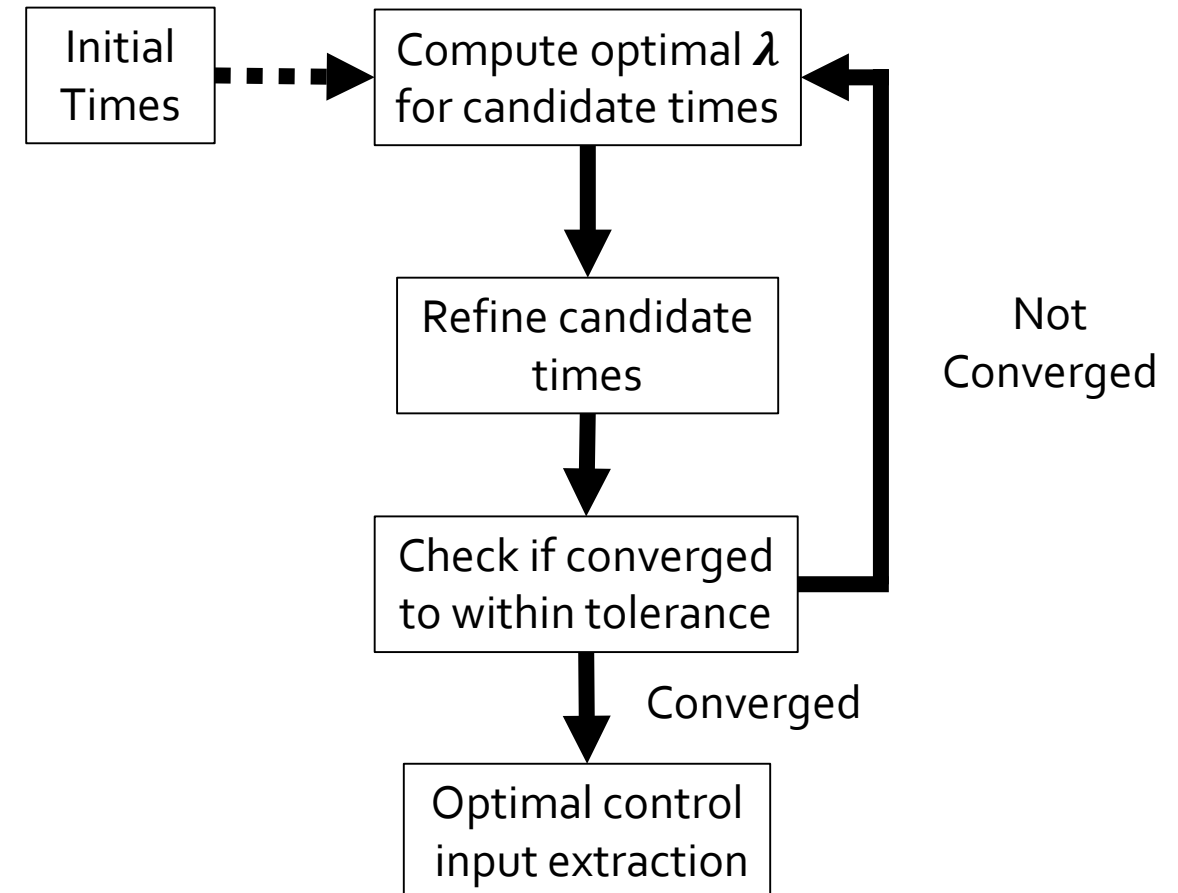
- Each λ defines a supporting hyperplane that is tangent to the reachable set
- Using multiple λ it is possible to compute an arbitrarily accurate polyhedral approximation of the reachable set
- User can trade between accuracy and computation cost



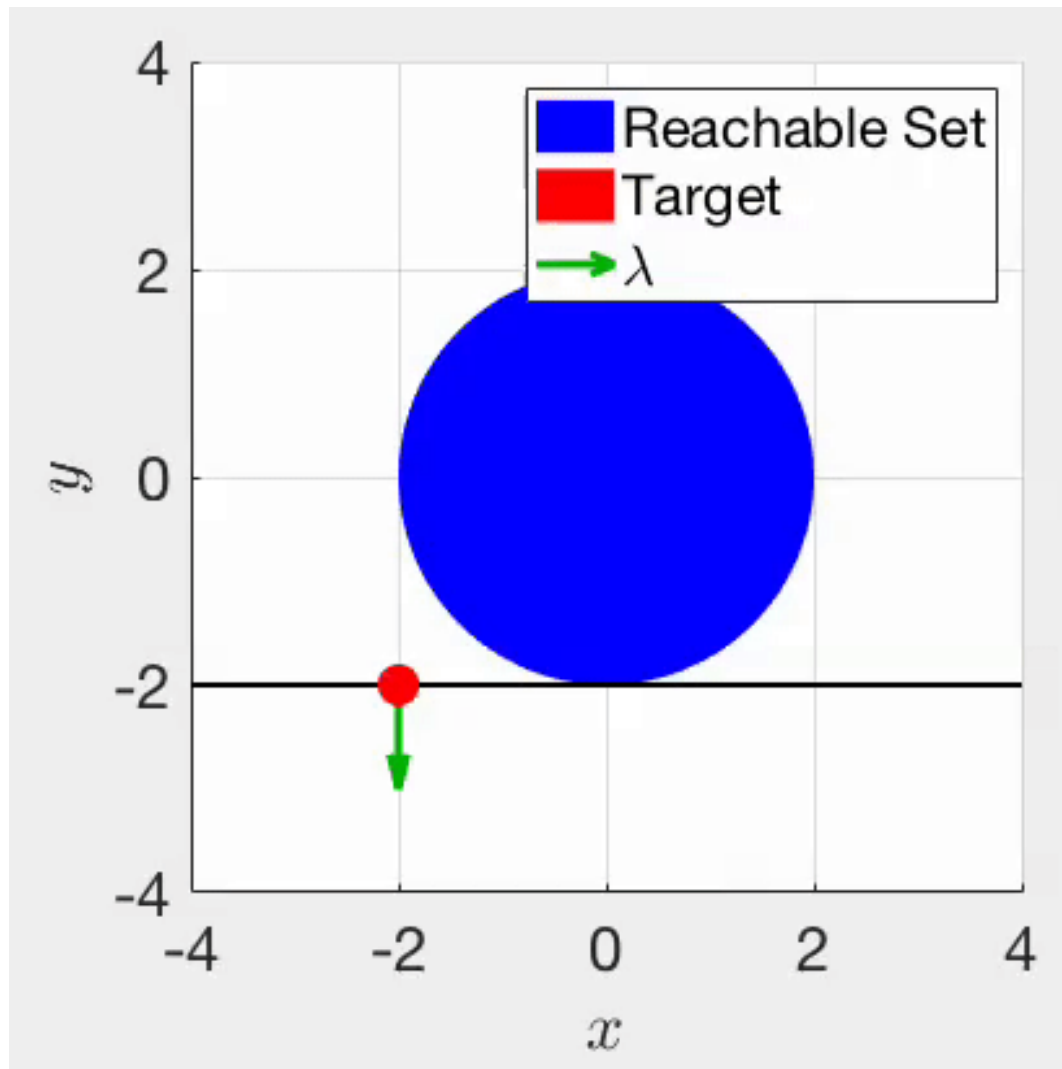
Example circumscribing polyhedra

Numerical Solution Method

- ↗ Generate initial set of candidate times
- ↗ Iteratively refine λ and candidate times until convergence criteria satisfied
- ↗ Extract optimal control inputs

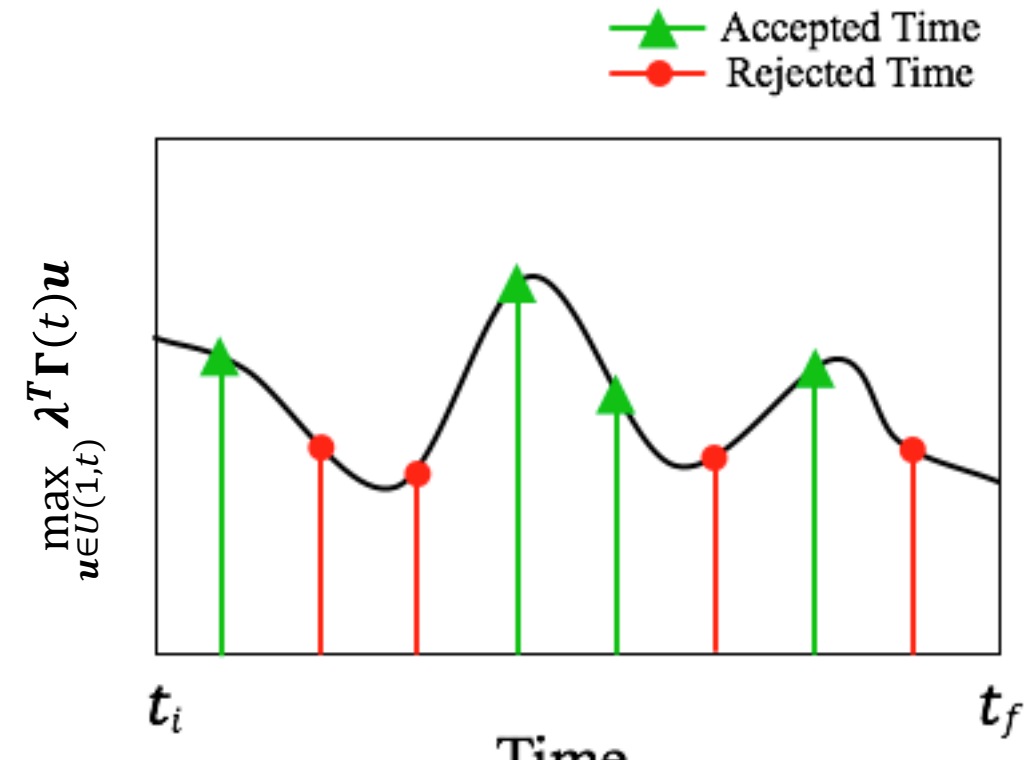


Numerical Solution Method



Generation of Initial Candidate Times

- ↗ Requirements: Target pseudostate can be reached by control inputs applied at specified times
- ↗ Option 1: Select times near local maxima of $\arg\max_{u \in U(1,t)} \lambda^T \Gamma(t) u$ for provided a-priori estimate of λ
- ↗ Option 2: Discretize admissible control window
- ↗ Best choice depends on behavior of solver w.r.t constraints



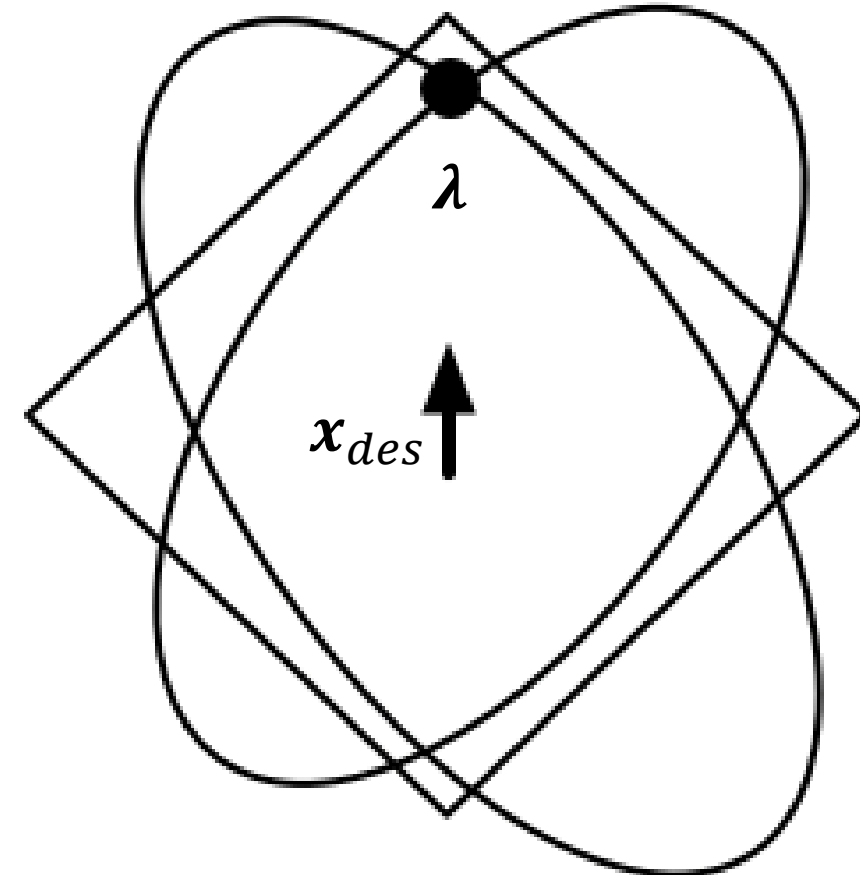
Iteration Procedure

- Step 1: Solve for optimal λ for specified set of candidate times

Maximize: $\lambda^T \mathbf{x}_{des}$

Subject to: $\max_{\mathbf{u} \in U(1,t)} \lambda^T \Gamma(t_j) \mathbf{u} \leq 1$
 $t_j \in T_{cand}$

$$\max_{\mathbf{u} \in U(1,t)} \lambda^T \Gamma(t_j) \mathbf{u} = 1$$

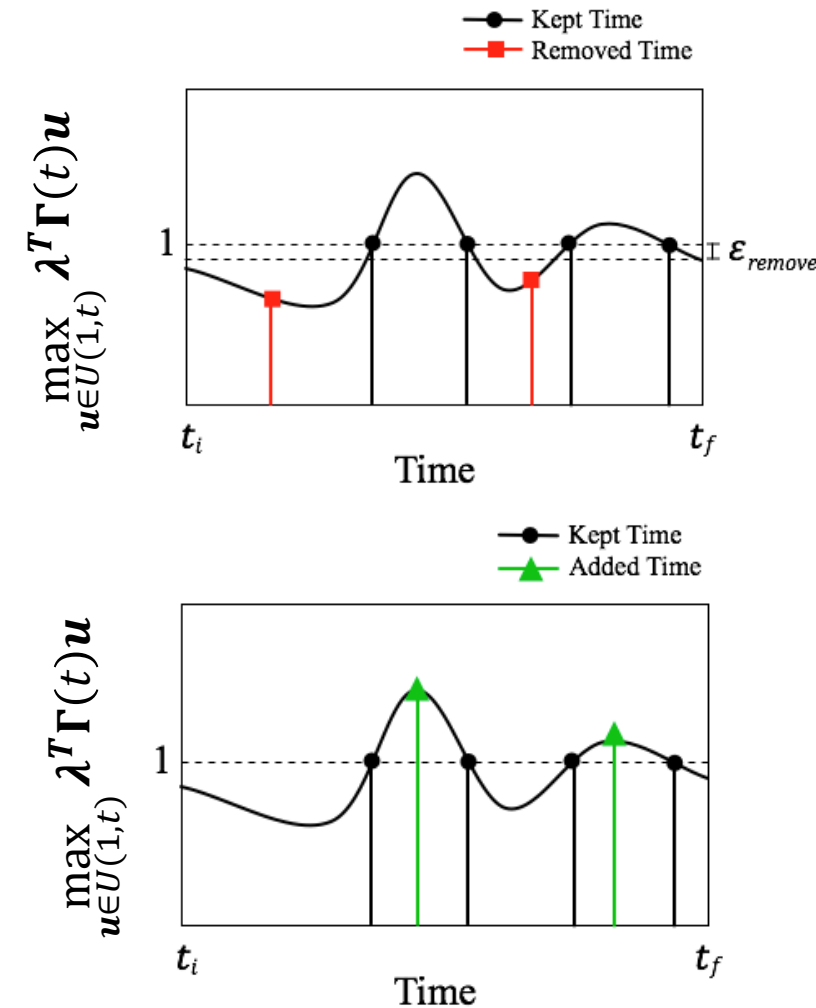


Iteration Procedure

- ↗ Step 2: Update set of candidate times based on new λ
 - ↗ Remove all times when

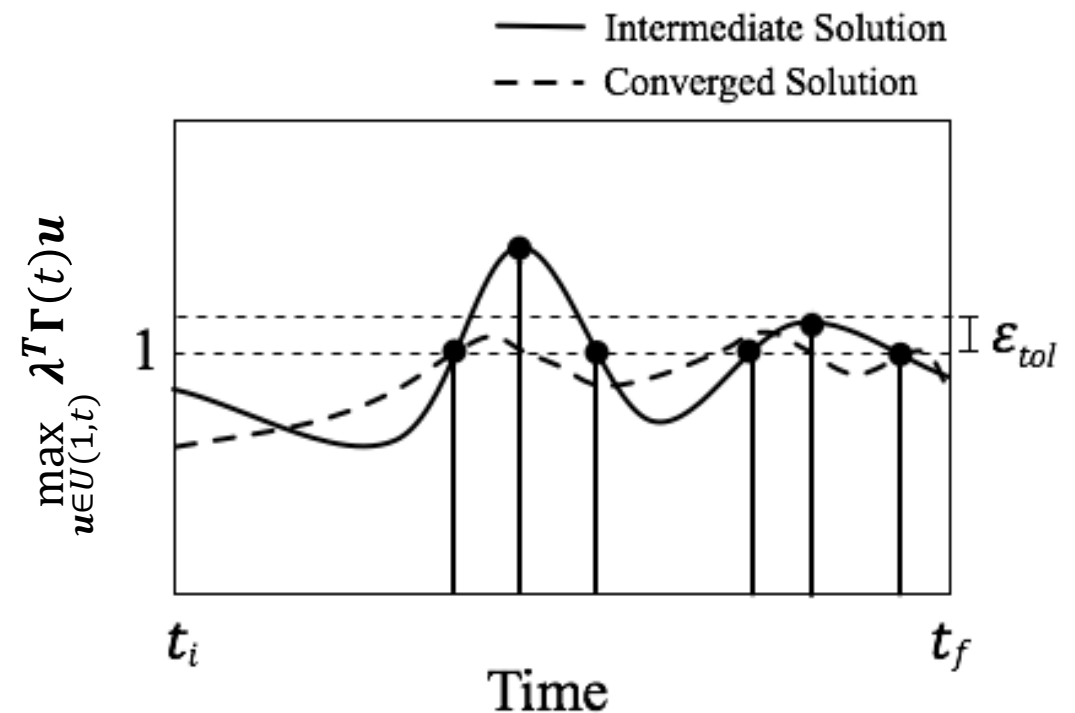
$$\max_{\mathbf{u} \in U(1,t)} \boldsymbol{\lambda}^T \boldsymbol{\Gamma}(t) \mathbf{u} < 1 - \varepsilon_{remove}$$
 - ↗ Add all local maxima of

$$\max_{\mathbf{u} \in U(1,t)} \boldsymbol{\lambda}^T \boldsymbol{\Gamma}(t) \mathbf{u}$$
 larger than 1



Convergence Criteria

- ↗ Terminate algorithm when difference between cost of feasible control input sequence and lower bound below specified threshold
- ↗ Lower bound: $\frac{\lambda^T x_{des}}{\max_{t \in T, u \in U(1,t)} \lambda^T \Gamma(t) u}$
- ↗ Feasible cost: $\lambda^T x_{des}$
- ↗ **Algorithm considered converged when**
$$\max_{t \in T, u \in U(1,t)} \lambda^T \Gamma(t) u \leq 1 + \varepsilon_{tol}$$



Control Input Extraction

- Step 1: Compute optimal control input directions from λ_{opt}

$$\hat{\mathbf{u}}_{opt}(t_j) = \underset{\mathbf{u} \in U(1, t_j)}{\operatorname{argmax}} \lambda_{opt}^T \Gamma(t_j) \mathbf{u}$$

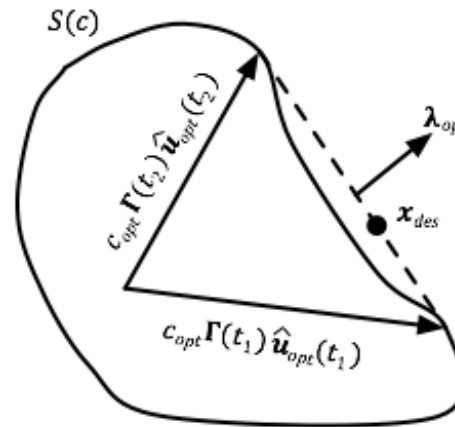
- Step 2: Compute corresponding pseudostate vectors

$$\mathbf{y}_j = \Gamma(t_j) \hat{\mathbf{u}}_{opt}(t_j)$$

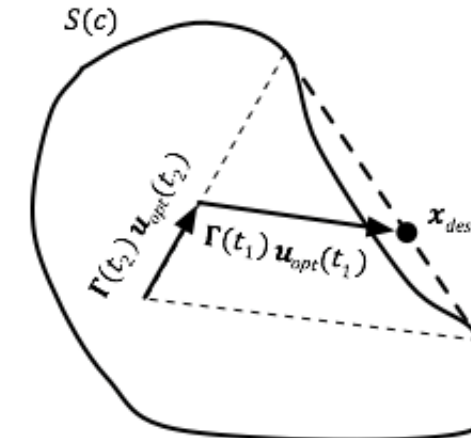
- Step 3: Compute optimal magnitudes

$$\text{Minimize: } \mathbf{x}_{err}^T Q \mathbf{x}_{err}$$

$$\text{Subject to: } \mathbf{x}_{err} = \mathbf{x}_{des} - \sum \alpha_j \mathbf{y}_j$$



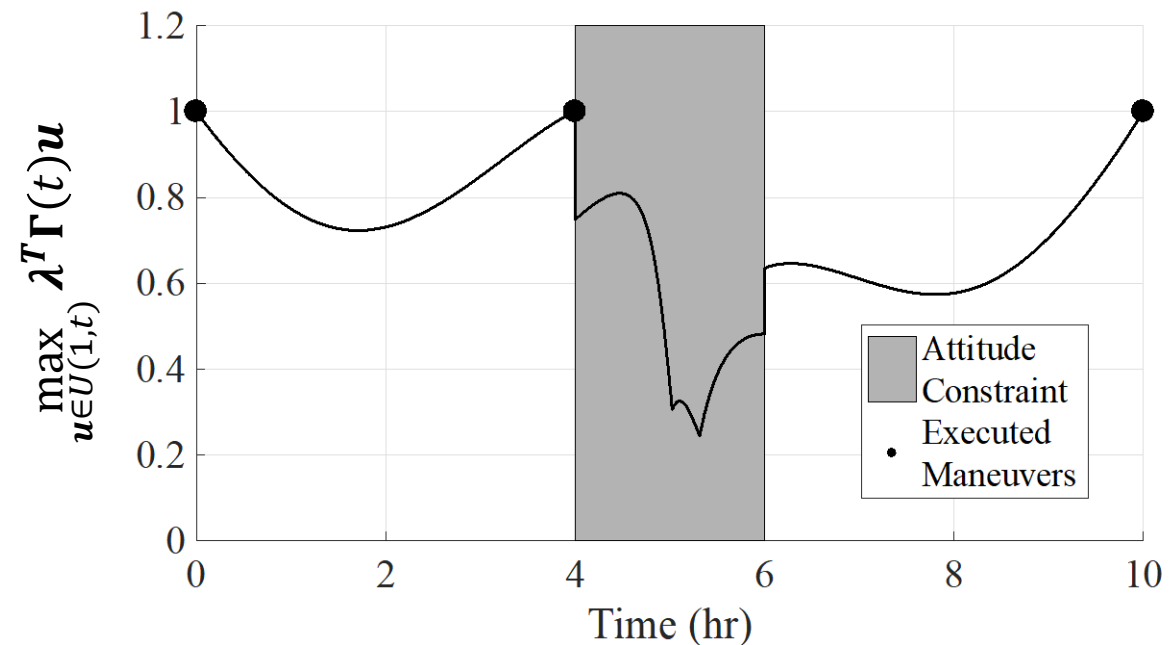
Computation of optimal control input directions



Computation of optimal control input magnitudes

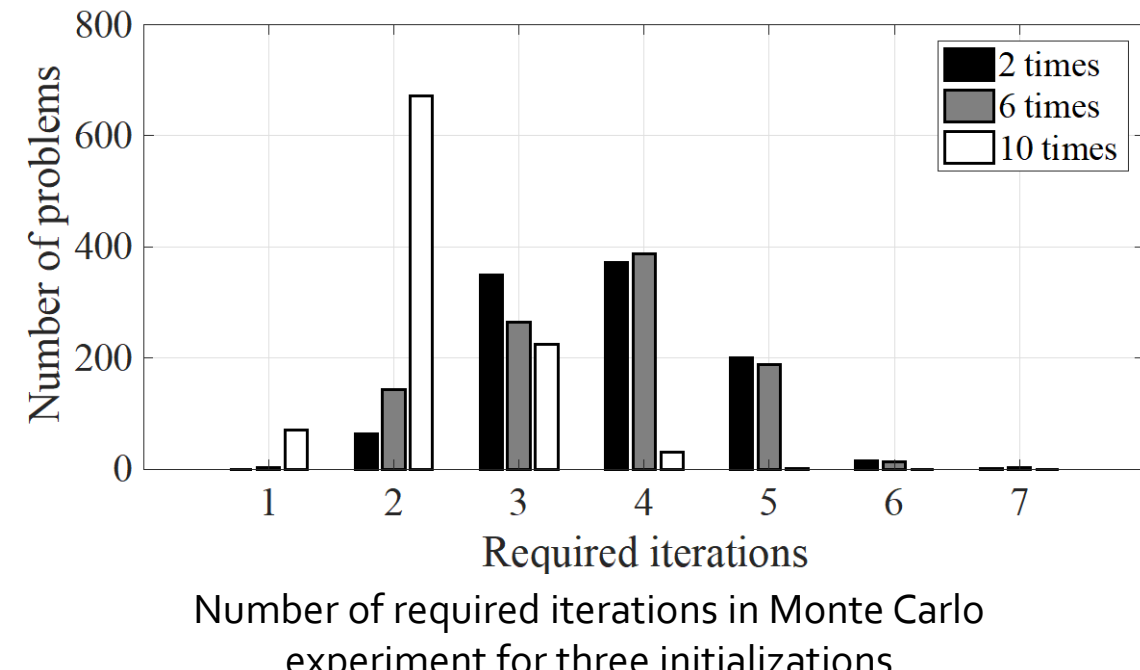
Example Problem

- ↗ Used algorithm to solve mDOT reconfiguration problem:
 - ↗ Less than 1 orbit
 - ↗ Eccentric, J_2 -perturbed orbit
 - ↗ Fixed attitude near perigee
 - ↗ Asymmetric thrusters
- ↗ Algorithm converged to 3-impulse solution in two iterations
 - ↗ All impulses have components in R, T, and N directions



Monte Carlo Experiment

- ↗ Solved 1000 reconfigurations based on mDOT with time-varying attitude constraints
- ↗ Solutions required to have total cost within 1% of global optimum
- ↗ Algorithm converged in 1-7 refinement iterations
- ↗ Algorithm was implemented on a Tyvak flatsat processor (800 MHz) with a run time of 3-10 seconds



Optimal Impulsive Control Review

1. Developed optimality criteria for broad class of linear impulsive optimal control problems using reachable sets
2. Derived computationally efficient lower bounds on minimum cost
3. Developed globally convergent, real-time algorithm that provides solutions within user-specified threshold of lower bound

AA 279D GUEST LECTURE

Adam W. Koenig

Stanford's Space Rendezvous Laboratory (SLAB)

slab.stanford.edu

